

Non-Hermitian Origin of Wannier Localizability and Detachable Topological Boundary States

Daichi Nakamura,^{1,*} Ken Shiozaki,^{2,†} Kenji Shimomura,² Masatoshi Sato,² and Kohei Kawabata^{1,‡}

¹*Institute for Solid State Physics, University of Tokyo, Kashiwa, Chiba 277-8581, Japan*

²*Center for Gravitational Physics and Quantum Information,*

Yukawa Institute for Theoretical Physics, Kyoto University, Kyoto 606-8502, Japan

(Dated: July 15, 2024)

While topology can impose obstructions to exponentially localized Wannier functions, certain topological insulators are exempt from such Wannier obstructions. The absence of the Wannier obstructions can further accompany topological boundary states that are detachable from the bulk bands. Here, we elucidate a close connection between these detachable topological boundary states and non-Hermitian topology. Identifying topological boundary states as non-Hermitian topology, we demonstrate that intrinsic non-Hermitian topology leads to the inevitable spectral flow. By contrast, we show that extrinsic non-Hermitian topology underlies the detachment of topological boundary states and clarify anti-Hermitian topology of the detached boundary states. Based on this connection and K -theory, we complete the tenfold classification of Wannier localizability and detachable topological boundary states.

Topological insulators and superconductors play a pivotal role in modern condensed matter physics [1, 2], generally classified by the fundamental tenfold internal symmetry classification [3–6]. A distinctive feature of the topologically non-trivial bulk bands is the emergence of anomalous states at boundaries. Additionally, certain topology, such as the Chern number, imposes obstructions to constructing exponentially localized Wannier functions in the bulk bands [7–11]. The Wannier localizability also provides a foundation of topological phases, including topological crystalline insulators [12]. Conversely, other types of topology do not necessarily lead to the Wannier obstructions [13–15]. Remarkably, as opposed to the conventional intuition of the bulk-boundary correspondence, such Wannier-localizable topological insulators have recently been shown to host boundary states that are detachable from the bulk bands [16, 17]. In this Letter, we reveal that these detachable topological boundary states originate from non-Hermitian topology.

Recently, topological characterization of non-Hermitian systems has attracted considerable interest [18–63]. Non-Hermiticity arises from exchange of energy and particles with the environment [64, 65], and yields various topological phenomena unique to open systems [66–81]. Importantly, these non-Hermitian topological phenomena stem from two types of complex-energy gaps: point and line gaps [36]. Non-Hermitian systems with point gaps are continuously deformable to unitary systems and thus can be intrinsic to non-Hermitian systems. Such intrinsic non-Hermitian topology gives rise to the skin effect [23, 30, 31, 42, 45, 46] and exceptional points [26, 29, 48, 55]. Conversely, non-Hermitian systems with real (imaginary) line gaps are continuously deformable to Hermitian (anti-Hermitian) systems and therefore have counterparts in conventional Hermitian systems. The interplay of point and line gaps enriches the topological classification of non-Hermitian systems based on the 38-fold internal symmetry classes [36].

In this Letter, we uncover a hidden relationship between non-Hermitian topology and Hermitian detachable topological boundary states. Associating topological boundary states

with point-gap topology, we demonstrate that intrinsic and extrinsic point-gap topology results in nondetachable and detachable topological boundary states, respectively. Utilizing this connection and K -theory, we complete the tenfold classification of Wannier localizability and detachable topological boundary states (Table I). We also elucidate topology of the detached boundary states, generally classified in Table II.

Non-Hermitian topology.—A distinctive feature of non-Hermitian systems is complex-valued spectra, leading to two types of complex-energy gaps: point and line gaps [29, 36]. In the presence of a point (line) gap, complex-energy bands do not cross a reference point (line) in the complex-energy plane. Specifically, a non-Hermitian Hamiltonian H is defined to have a point gap for $E_n \neq E_P$, where E_n 's are complex eigenenergies of H , and $E_P \in \mathbb{C}$ is a reference energy. By contrast, H is defined to have a real (imaginary) line gap for $\text{Re } E_n \neq E_L$ ($\text{Im } E_n \neq E_L$) with $E_L \in \mathbb{R}$, implying separable bands [26].

The interplay of point and line gaps enriches the topological classification and bulk-boundary correspondence of non-Hermitian systems [36]. Even if a point gap is open, a line gap is not necessarily open. However, a point gap is always open when a line gap is open by placing a reference point on the reference line. Consequently, some point-gap topology is continuously deformable to line-gap topology and therefore has a counterpart in Hermitian or anti-Hermitian systems. In contrast to such extrinsic non-Hermitian topology, some point-gap topology is irreducible to line-gap topology and thus intrinsic to non-Hermitian systems.

Chiral edge state and intrinsic non-Hermitian topology.—To illustrate the role of intrinsic non-Hermitian topology in nondetachable topological boundary states, we investigate a chiral edge state in a two-dimensional Chern insulator: $H(k_x) = k_x$. In the adiabatic change of momentum, the chiral edge state exhibits a spectral flow from negative infinity to positive infinity, inevitably requiring the attachment to the bulk degrees of freedom.

We identify the chiral edge state with a point-gapped non-

TABLE I. Wannier localizability of the d -dimensional bulk and detachability of $(d - 1)$ -dimensional boundary states in topological insulators and superconductors. The tenfold Altland-Zirnbauer symmetry classes consist of time-reversal symmetry (TRS), particle-hole symmetry (PHS), and chiral symmetry (CS). The entries with “ \checkmark ” (“ \times ”) accompany the Wannier nonlocalizable (localizable) topological phases in the bulk and exhibit nondetachable (detachable) boundary states with intrinsic (extrinsic) non-Hermitian topology. The entries with “ \checkmark/\times ” specify the Wannier nonlocalizable and localizable topological phases for the odd and even numbers of topological invariants, respectively.

Class	TRS	PHS	CS	$d = 1$	$d = 2$	$d = 3$	$d = 4$	$d = 5$	$d = 6$	$d = 7$	$d = 8$
A	0	0	0	0	\mathbb{Z}^{\checkmark}	0	\mathbb{Z}^{\checkmark}	0	\mathbb{Z}^{\checkmark}	0	\mathbb{Z}^{\checkmark}
AIII	0	0	1	\mathbb{Z}^{\times}	0	\mathbb{Z}^{\times}	0	\mathbb{Z}^{\times}	0	\mathbb{Z}^{\times}	0
AI	+1	0	0	0	0	0	$2\mathbb{Z}^{\checkmark}$	0	$\mathbb{Z}_2^{\checkmark}$	$\mathbb{Z}_2^{\checkmark}$	\mathbb{Z}^{\checkmark}
BDI	+1	+1	1	\mathbb{Z}^{\times}	0	0	0	$2\mathbb{Z}^{\times}$	0	\mathbb{Z}_2^{\times}	\mathbb{Z}_2^{\times}
D	0	+1	0	\mathbb{Z}_2^{\times}	\mathbb{Z}^{\checkmark}	0	0	0	$2\mathbb{Z}^{\checkmark}$	0	\mathbb{Z}_2^{\times}
DIII	-1	+1	1	\mathbb{Z}_2^{\times}	$\mathbb{Z}_2^{\checkmark}$	$\mathbb{Z}^{\checkmark}/\times$	0	0	0	$2\mathbb{Z}^{\times}$	0
AII	-1	0	0	0	$\mathbb{Z}_2^{\checkmark}$	$\mathbb{Z}_2^{\checkmark}$	\mathbb{Z}^{\checkmark}	0	0	0	$2\mathbb{Z}^{\checkmark}$
CII	-1	-1	1	$2\mathbb{Z}^{\times}$	0	\mathbb{Z}_2^{\times}	\mathbb{Z}_2^{\times}	\mathbb{Z}^{\times}	0	0	0
C	0	-1	0	0	$2\mathbb{Z}^{\checkmark}$	0	\mathbb{Z}_2^{\times}	\mathbb{Z}_2^{\times}	\mathbb{Z}^{\checkmark}	0	0
CI	+1	-1	1	0	0	$2\mathbb{Z}^{\times}$	0	\mathbb{Z}_2^{\times}	$\mathbb{Z}_2^{\checkmark}$	$\mathbb{Z}^{\checkmark}/\times$	0

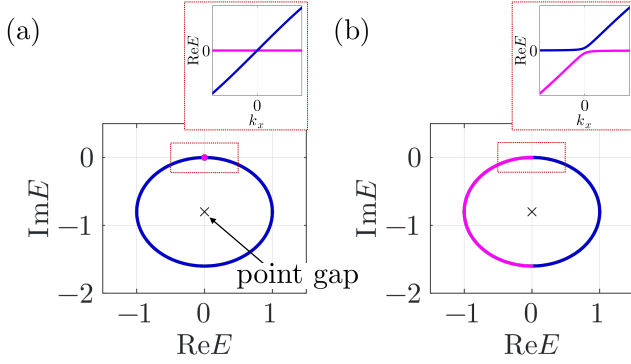


FIG. 1. Intrinsic non-Hermitian topology of the chiral edge state. Complex spectrum of the point-gapped non-Hermitian model $\tilde{H}_A(k_x)$ in Eq. (3) ($\gamma = 0.8$) for (a) $v = 0$ and (b) $v = 0.03$. (a) Around $E = 0$, $\tilde{H}_A(k)$ reduces to the chiral edge state $E(k_x) \simeq k_x$ (inset). (b) The perturbation $v \neq 0$ leads to a swap of two complex bands (blue and magenta curves), protecting the spectral flow.

Hermitian system [Fig. 1 (a)],

$$H_A(k_x) = \sin k_x + i\gamma(\cos k_x - 1), \quad (1)$$

where $\gamma > 0$ is the degree of non-Hermiticity and describes the nonreciprocal hopping in real space [82]. This identification is formalized by adding dissipation to the edges [58–60]. The non-Hermitian term can also be understood as the coupling between the bulk and edges [61], where the bulk degrees of freedom at infinity correspond to decaying eigenstates with $\text{Im} E < 0$. Around the Fermi surface $\text{Re} E = 0$, this non-Hermitian system $H_A(k_x)$ hosts two modes k_x and $-k_x - 2i\gamma$, only the former of which survives since the latter decays with a finite lifetime $1/2\gamma$ [43, 47].

This identification is generally guaranteed by point-gap

topology [29, 36], i.e.,

$$W_1[H - E_P] := - \oint_{\text{BZ}} \frac{dk}{2\pi i} \left(\frac{d}{dk} \log \det [H(k) - E_P] \right). \quad (2)$$

The non-Hermitian system $H_A(k_x)$ in Eq. (1) is characterized by $W_1[H_A - E_P] = 1$ for the reference energy E_P inside the loop of the complex spectrum. Importantly, this complex-spectral winding always vanishes for Hermitian systems and hence intrinsic to non-Hermitian systems. Thus, the point gap cannot be opened or reduced to any line gaps while preserving the point-gap topology. Consequently, the chiral edge state around $E = 0$ cannot be detached from other eigenstates with $\text{Im} E < 0$ that play a role of the bulk degree of freedom. To further confirm this stability, we couple the chiral edge state to a trivial band $H = 0$,

$$\tilde{H}_A(k_x) = \begin{pmatrix} H_A(k_x) & v \\ v^* & 0 \end{pmatrix}, \quad (3)$$

with the coupling amplitude $v \in \mathbb{C}$. As momentum is traversed through the Brillouin zone, the perturbed complex two bands swap with each other, forbidding the point-gap opening [Fig. 1 (b)].

Dirac surface state and extrinsic non-Hermitian topology.—In contrast to the chiral edge states, we demonstrate that the detachable topological boundary states accompany extrinsic non-Hermitian topology. As a prime example, we investigate a Dirac surface state of a three-dimensional topological insulator protected solely by chiral symmetry: $H(\mathbf{k}) = k_x\sigma_x + k_y\sigma_y$. This Dirac Hamiltonian indeed respects chiral symmetry $\Gamma H(\mathbf{k})\Gamma^{-1} = -H(\mathbf{k})$ with $\Gamma = \sigma_z$ and hence belongs to class AIII. Since chiral symmetry is relevant only to zero energy, $H(\mathbf{k})$ accompanies no spectral flow and hence is detachable from the bulk bands [17, 83].

We identify this Dirac surface state as a point-gapped non-

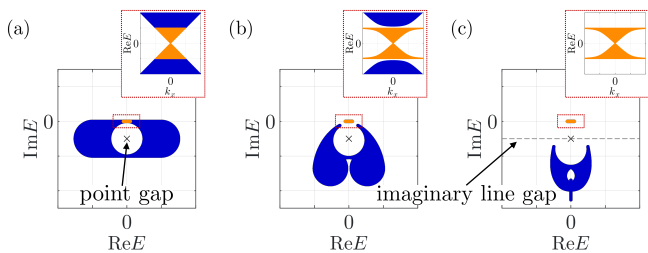


FIG. 2. Detachment of topological boundary states in three-dimensional topological insulators protected by chiral symmetry (class AIII). (a) The Dirac surface state (inset) is identified as a chiral-symmetric non-Hermitian system with point-gap topology (main panel). (b, c) Owing to the extrinsic nature of the point-gap topology, chiral-symmetry-preserving perturbations open an imaginary line gap (dashed line) while preserving the point gap. The Dirac surface state around $E = 0$ is separated from the other decaying bands with $\text{Im } E < 0$, corresponding to the detachment from the bulk bands.

Hermitian system in two dimensions,

$$H_{\text{AIII}}(\mathbf{k}) = (\sin k_x) \sigma_x + (1 - \cos k_x - \cos k_y) \sigma_y + i\gamma (\sin k_y - 1), \quad (4)$$

with $\gamma > 0$. This non-Hermitian Dirac model also respects chiral symmetry [36]:

$$\Gamma H_{\text{AIII}}^\dagger(\mathbf{k}) \Gamma^{-1} = -H_{\text{AIII}}(\mathbf{k}) \quad (5)$$

with $\Gamma = \sigma_z$. Around the Fermi surface $\text{Re } E = 0$ (i.e., $k_x = 0$, $k_y = \pm\pi/2$), it comprises two modes, $k_x\sigma_x + k_y\sigma_y$ and $k_x\sigma_x - k_y\sigma_y - 2i\gamma$, only the former of which survives and reduces to the Hermitian Dirac surface state [43, 47].

Point-gap topology of this chiral-symmetric non-Hermitian Dirac model is captured by the (first) Chern number of the Hermitian matrix $i[H_{\text{AIII}}(\mathbf{k}) - E_P]\Gamma$, where the reference point E_P is chosen to respect chiral symmetry (i.e., $E_P \in i\mathbb{R}$) [36]. From the bulk-boundary correspondence, this boundary point-gap topology further coincides with the three-dimensional winding number $W_3[H_{\text{AIII}}^{\text{bulk}}]$ of the bulk:

$$\text{Ch}_1[i[H_{\text{AIII}} - E_P]\Gamma] = W_3[H_{\text{AIII}}^{\text{bulk}}]. \quad (6)$$

A crucial distinction from the chiral edge state is that this point-gap topology is continuously deformable to imaginary-line-gap topology while preserving the point gap and chiral symmetry (Fig. 2). In fact, when we couple $H_{\text{AIII}}(\mathbf{k})$ to a trivial band $H = \varepsilon\sigma_x$ ($\varepsilon \geq 0$) by

$$\tilde{H}_{\text{AIII}}(\mathbf{k}) = \begin{pmatrix} H_{\text{AIII}}(\mathbf{k}) & v\sigma_- \\ v^*\sigma_+ & \varepsilon\sigma_x \end{pmatrix} \quad (7)$$

with $v \in \mathbb{C}$, the bands around $E = 0$ are separated from the other bands with $\text{Im } E < 0$, leading to the opening of an imaginary line gap. As discussed above, decaying eigenstates $\text{Im } E < 0$ describe the bulk degrees of freedom. Thus, the imaginary-line-gap opening indicates the detachment of the Dirac surface state from the bulk bands.

Once the boundary states are detached from the bulk bands, we can introduce a projector to the detached boundary Hamiltonian $H_{\text{boundary}}(\mathbf{k})$ by

$$P_{\text{boundary}}(\mathbf{k}) := \oint_C \frac{dE}{2\pi i} \frac{1}{E - H_{\text{boundary}}(\mathbf{k})}, \quad (8)$$

where C is chosen to be a symmetry-preserving loop in the complex energy plane that encloses the boundary bands [see, for example, the red dotted rectangle in Fig. 2 (c)]. Notably, chiral symmetry in Eq. (5) behaves like \mathbb{Z}_2 unitary symmetry that commutes with $P_{\text{boundary}}(\mathbf{k})$ [84]. Hence, $P_{\text{boundary}}(\mathbf{k})$ hosts two independent Chern numbers $\text{Ch}_1[P_{\text{boundary}}^{(\pm)}]$ in the subspaces of $\Gamma = \pm 1$. This $\mathbb{Z} \oplus \mathbb{Z}$ topological classification for imaginary line gaps includes the \mathbb{Z} classification for point gaps, showing the extrinsic nature of the point-gap topology. Specifically, a map from $\mathbb{Z} \oplus \mathbb{Z}$ to \mathbb{Z} is given as [46, 83, 85]

$$\text{Ch}_1[P_{\text{boundary}}^{(+)}] - \text{Ch}_1[P_{\text{boundary}}^{(-)}] = \text{Ch}_1[iH_{\text{AIII}}\Gamma], \quad (9)$$

where a reference point and line are chosen appropriately. Thus, in combination with Eq. (6), as a direct consequence of the bulk topology $W_3[H_{\text{AIII}}^{\text{bulk}}] \neq 0$, the detached boundary states inevitably exhibit the nontrivial Chern number $\text{Ch}_1[P^{(+)}] \neq 0$ or $\text{Ch}_1[P^{(-)}] \neq 0$, consistent with the surface Chern number introduced in Refs. [16, 17]. Notably, using this general discussion, we systematically classify potential nontrivial topology of detached boundary states (Table II), as discussed below.

Classification.—While we have hitherto investigated the prototypical models, our formulation is generally applicable to topological insulators and superconductors, leading to the classification of Wannier localizability and detachable topological boundary states in Table I. First, we generally identify topological boundary states as non-Hermitian systems with point-gap topology [43, 47]. There, the Altland-Zirnbauer symmetry for original Hermitian systems reduces to the Altland-Zirnbauer[†] symmetry for non-Hermitian systems [36], based on chiral symmetry in Eq. (5), as well as time-reversal symmetry[†] and particle-hole symmetry[†],

$$\mathcal{T}H^T(\mathbf{k})\mathcal{T}^{-1} = H(-\mathbf{k}), \quad \mathcal{C}H^*(\mathbf{k})\mathcal{C}^{-1} = -H(-\mathbf{k}), \quad (10)$$

with unitary matrices \mathcal{T} and \mathcal{C} . This identification is generally applicable as long as point-gap topology is preserved.

Then, the detachability of the topological boundary states reduces to whether the corresponding point-gap topology is intrinsic. This is classified based on homomorphisms from imaginary-line-gap topology to point-gap topology [46, 83, 85, 86]. According to our classification, all the topological boundary states in the Wigner-Dyson classes (i.e., classes A, AI, and AII) cannot be detached from the bulk bands, consistent with their spectral flow [87]. Furthermore, as a direct consequence of the bulk topology in the chiral or Bogolioubov-de Gennes classes, the detached boundary states exhibit imaginary-line-gap topology, as summarized in Table II. Similarly to the three-dimensional bulk in class AIII,

TABLE II. Correspondence of topological invariants (top. invs.) between the d -dimensional bulk and $(d-1)$ -dimensional detached boundary (bdy). The symmetry classes are specified for the bulk. \mathbb{Z} invariants W for the symmetry classes accompanying chiral symmetry (i.e., classes AIII, BDI, DIII, CII, and CI), and \mathbb{Z}_2 invariants ν for the chiral and Bogoliubov-de Gennes classes.

Class	$(d-1)$ -dim. boundary top. inv. = d -dim. bulk top. inv.
Chiral	$\text{Ch}_n [P_{\text{bdy}}^{(+)}] - \text{Ch}_n [P_{\text{bdy}}^{(-)}] = W_{2n+1} [H_{\text{bulk}}]$
BDI	$\nu_{\text{AI}}^{d-1=8n+6} [P_{\text{bdy}}] = \nu_{\text{BDI}}^{d=8n+7} [H_{\text{bulk}}]$
BDI & D	$\nu_{\text{AI}}^{d-1=8n+7} [P_{\text{bdy}}] = \nu_{\text{BDI\&D}}^{d=8n+8} [H_{\text{bulk}}]$
D	$\text{Ch}_{4n} [P_{\text{bdy}}] \equiv \nu_{\text{D}}^{d=8n+1} [H_{\text{bulk}}] \pmod{2}$
DIII	$\frac{1}{2} \text{Ch}_{4n} [P_{\text{bdy}}] \equiv \nu_{\text{DIII}}^{d=8n+1} [H_{\text{bulk}}] \pmod{2}$
CII	$\nu_{\text{AII}}^{d-1=8n+2} [P_{\text{bdy}}] = \nu_{\text{CII}}^{d=8n+3} [H_{\text{bulk}}]$
C & CII	$\nu_{\text{AII}}^{d-1=8n+3} [P_{\text{bdy}}] = \nu_{\text{C\&CII}}^{d=8n+4} [H_{\text{bulk}}]$
C	$\text{Ch}_{4n+2} [P_{\text{bdy}}] \equiv \nu_{\text{C}}^{d=8n+5} [H_{\text{bulk}}] \pmod{2}$
CI	$\frac{1}{2} \text{Ch}_{4n+2} [P_{\text{bdy}}] \equiv \nu_{\text{CI}}^{d=8n+5} [H_{\text{bulk}}] \pmod{2}$

the boundary topology is captured by its projector in Eq. (8), for which particle-hole symmetry behaves like time-reversal symmetry [i.e., $\mathcal{C}P^*(\mathbf{k})\mathcal{C}^{-1} = P(-\mathbf{k})$]. Notably, such a projector can be introduced even for Hermitian detached boundary states [88].

Our classification also predicts other possible topological phases that host detachable boundary states. For example, surface states in three-dimensional \mathbb{Z}_2 topological insulators for class CII are also detachable from the bulk bands. As an advantage of our formalism, topology of the detached boundary states is systematically identified based on the classification with respect to imaginary line gaps. Specifically, particle-hole symmetry in the original space behaves like time-reversal symmetry in the projected subspace of the detached surface states in class CII, leading to the \mathbb{Z}_2 Kane-Mele or Fu-Kane topological invariant (see also Table II) [6, 89–92]. Similarly, in four dimensions, topological boundary states in the Wigner-Dyson classes cannot be separated from the bulk, while those in the chiral and Bogoliubov-de Gennes classes (i.e., classes CII and C) are detachable. Additionally, in classes DIII and CI, since particle-hole transformation flips chirality, the bulk winding number $W_{2n+1} [H_{\text{bulk}}]$ should be even if the boundary states are detached, resulting in the “ $\mathbb{Z}^{\checkmark}/\times$ classification” in Table I.

Wannier localizability.—Using K -theory, we clarify the relationship between the detachability of topological boundary states and Wannier localizability. For a gapped d -dimensional Hermitian system, we consider the bulk Hamiltonian $H(\mathbf{k})$ with the periodic boundary conditions and the boundary Hamiltonian $\hat{H}(\mathbf{k}_{\parallel})$ with the semi-infinite boundary conditions, which are classified by the degree-0 and degree- $(+1)$ K -groups $\phi K_G^{(\tau,c)+0}(T^d)$ and $\phi K_G^{(\tau,c)+1}(T^{d-1})$, respectively [93–98]. The bulk-boundary correspondence is denoted by $f_G^{\text{BBC}} : \phi K_G^{(\tau,c)+0}(T^d) \ni [H(\mathbf{k})] \mapsto [\hat{H}(\mathbf{k}_{\parallel})] \in \phi K_G^{(\tau,c)+1}(T^{d-1})$, where T^d and T^{d-1} are respectively the

bulk and boundary Brillouin zone tori, G is the symmetry group that is compatible with the boundary and possibly includes crystalline symmetry, and $c : G \rightarrow \mathbb{Z}_2$ is the homomorphism specifying whether $g \in G$ is symmetry or antisymmetry such as particle-hole and chiral symmetries.

Similarly to the previous procedures, we map the boundary Hermitian Hamiltonian $\hat{H}(\mathbf{k}_{\parallel})$ to a point-gapped non-Hermitian Hamiltonian $H_{\text{P}}(\mathbf{k}_{\parallel}) := i \exp[-i\chi(\hat{H}(\mathbf{k}_{\parallel}))]$, with a continuous function $\chi(E)$ that satisfies $\chi(E) = \text{sgn}(E)$ for $|E| > E_{\text{gap}}$ and $\chi(E) = E/E_{\text{gap}}$ for $|E| \leq E_{\text{gap}}$ with the bulk gap $E_{\text{gap}} > 0$. The detachment of $\hat{H}(\mathbf{k}_{\parallel})$ corresponds to imposing an imaginary line gap on $H_{\text{P}}(\mathbf{k}_{\parallel})$, which is further formulated by the anti-Hermitian condition for $H_{\text{P}}(\mathbf{k}_{\parallel})$ [i.e., $H_{\text{P}}^{\dagger}(\mathbf{k}_{\parallel}) = -H_{\text{P}}(\mathbf{k}_{\parallel})$] [46]. Notably, antisymmetries for $H_{\text{P}}(\mathbf{k}_{\parallel})$ behave as symmetries for $iH_{\text{P}}(\mathbf{k}_{\parallel})$, and eventually, the imaginary-line-gapped phases are classified by the degree-0 K -group with trivial c [i.e., $\phi K_G^{(\tau,c_{\text{triv}})+0}(T^{d-1})$]. If G includes antisymmetry, we have the following commutative diagram [83]:

$$\begin{array}{ccc}
 & & \phi K_G^{(\tau,c_{\text{triv}})+0}(T^{d-1}) \\
 & & \downarrow f_{L_i}^{\text{bdy}} \\
 \phi K_G^{(\tau,c)+0}(T^d) & \xrightarrow{f_G^{\text{BBC}}} & \phi K_G^{(\tau,c)+1}(T^{d-1}) \quad (11) \\
 \downarrow f_0^{\text{bulk}} & & \downarrow f_0^{\text{bdy}} \\
 \phi K_{G_0}^{\tau+0}(T^d) & \xrightarrow{f_{G_0}^{\text{BBC}}} & \phi K_{G_0}^{\tau+1}(T^{d-1})
 \end{array}$$

Here, $G_0 \subsetneq G$ is the subgroup excluding antisymmetries, the K -groups $\phi K_{G_0}^{\tau+0}(T^d)$ and $\phi K_{G_0}^{\tau+1}(T^{d-1})$ respectively classify the bulk and boundary Hamiltonians protected only by G_0 , and f_0^{bulk} and f_0^{bdy} are defined by forgetting antisymmetries. The right vertical line in Eq. (11) is exact, and $f_{L_i}^{\text{bdy}}$ maps imaginary-line-gapped phases to point-gapped phases [46]. Saliiently, the exactness $\text{im } f_{L_i}^{\text{bdy}} = \ker f_0^{\text{bdy}}$ indicates that the boundary Hamiltonian $\hat{H}(\mathbf{k}_{\parallel})$ is detachable and exhibits no spectral flow ($[\hat{H}(\mathbf{k}_{\parallel})] \in \text{im } f_{L_i}$) if and only if $\hat{H}(\mathbf{k}_{\parallel})$ is gappable ($[\hat{H}(\mathbf{k}_{\parallel})] \in \ker f_0$) when ignoring antisymmetries.

Suppose that the bulk Hamiltonian $H(\mathbf{k})$ exhibits the spectral flow on the boundary, expressed as $f_G^{\text{BBC}}([H(\mathbf{k})]) \notin \text{im } f_{L_i}^{\text{bdy}}$. Then, the diagram in Eq. (11) implies that $H(\mathbf{k})$ exhibits a nontrivial topological invariant in the K -group $\phi K_{G_0}^{\tau+0}(T^d)$, which obstructs the existence of localized Wannier states. This aligns with the fact that if a real-space boundary hosts a spectral flow, either occupied or unoccupied Bloch states are no longer Wannier localizable [17]. Notably, such a boundary includes cylindrical or spherical boundaries that can realize higher-order topological boundary states. Furthermore, Table I is consistent with the symmetry-forgetting homomorphisms f_0^{bdy} for the tenfold Altland-Zirnbauer symmetry classes [83].

Discussions.—In this Letter, we elucidate that non-Hermitian topology underlies Wannier localizability and de-

tachable boundary states in Hermitian topological insulators and superconductors, thereby establishing their classification (Table I). Specifically, we demonstrate that while intrinsic non-Hermitian topology prohibits the detachment of topological boundary states, extrinsic non-Hermitian topology permits it and further leads to anti-Hermitian topology of the detached boundary states. Our formulation reveals that the detached topological boundary states concomitantly exhibit Wigner-Dyson-type gapped topology in total and chiral-type or Bogoliubov-de Gennes-type gapless topology at zero energy. They should exhibit unique Anderson localization and transitions, meriting further investigation. Additionally, our formulation is applicable to topological crystalline insulators. As a prime example, we investigate reflection-invariant second-order topological insulators [83, 99–102]. It is also worthwhile to extend our formulation to detachable boundary states in other types of topological insulators, such as Hopf insulators [16, 103] and nonsymmorphic insulators [104, 105].

Note added.—After the completion of this work, we became aware of a recent related work [106].

We thank Akira Furusaki, Shingo Kobayashi, and Shinsei Ryu for helpful discussion. We appreciate the long-term workshop “Recent Developments and Challenges in Topological Phases” (YITP-T-24-03) held at Yukawa Institute for Theoretical Physics (YITP), Kyoto University. D.N., K. Shiozaki, K. Shimomura, and M.S. are supported by JST CREST Grant No. JPMJCR19T2. K. Shiozaki is supported by JSPS KAKENHI Grant Nos. 22H05118 and 23H01097. K. Shimomura is supported by JST SPRING, Grant No. JPMJSP2110. M.S. is supported by JSPS KAKENHI Grant No. 24K00569. K.K. is supported by MEXT KAKENHI Grant-in-Aid for Transformative Research Areas A “Extreme Universe” No. 24H00945.

* daichi.nakamura@issp.u-tokyo.ac.jp

† ken.shiozaki@yukawa.kyoto-u.ac.jp

‡ kawabata@issp.u-tokyo.ac.jp

- [1] M. Z. Hasan and C. L. Kane, Colloquium: Topological insulators, *Rev. Mod. Phys.* **82**, 3045 (2010).
- [2] X.-L. Qi and S.-C. Zhang, Topological insulators and superconductors, *Rev. Mod. Phys.* **83**, 1057 (2011).
- [3] A. Altland and M. R. Zirnbauer, Nonstandard symmetry classes in mesoscopic normal-superconducting hybrid structures, *Phys. Rev. B* **55**, 1142 (1997).
- [4] A. P. Schnyder, S. Ryu, A. Furusaki, and A. W. W. Ludwig, Classification of topological insulators and superconductors in three spatial dimensions, *Phys. Rev. B* **78**, 195125 (2008); S. Ryu, A. P. Schnyder, A. Furusaki, and A. W. W. Ludwig, Topological insulators and superconductors: tenfold way and dimensional hierarchy, *New J. Phys.* **12**, 065010 (2010).
- [5] A. Kitaev, Periodic table for topological insulators and superconductors, *AIP Conf. Proc.* **1134**, 22 (2009).
- [6] C.-K. Chiu, J. C. Y. Teo, A. P. Schnyder, and S. Ryu, Classification of topological quantum matter with symmetries, *Rev. Mod. Phys.* **88**, 035005 (2016).
- [7] D. J. Thouless, Wannier functions for magnetic sub-bands, *J. Phys. C* **17**, L325 (1984).
- [8] C. Brouder, G. Panati, M. Calandra, C. Mourougane, and N. Marzari, Exponential Localization of Wannier Functions in Insulators, *Phys. Rev. Lett.* **98**, 046402 (2007).
- [9] A. A. Soluyanov and D. Vanderbilt, Wannier representation of \mathbb{Z}_2 topological insulators, *Phys. Rev. B* **83**, 035108 (2011).
- [10] N. Read, Compactly supported Wannier functions and algebraic K -theory, *Phys. Rev. B* **95**, 115309 (2017).
- [11] D. Vanderbilt, *Berry Phases in Electronic Structure Theory: Electric Polarization, Orbital Magnetization and Topological Insulators* (Cambridge University Press, Cambridge, 2018).
- [12] H. C. Po, H. Watanabe, and A. Vishwanath, Fragile Topology and Wannier Obstructions, *Phys. Rev. Lett.* **121**, 126402 (2018).
- [13] W. Kohn, Analytic Properties of Bloch Waves and Wannier Functions, *Phys. Rev.* **115**, 809 (1959).
- [14] S. Kivelson, Wannier functions in one-dimensional disordered systems: Application to fractionally charged solitons, *Phys. Rev. B* **26**, 4269 (1982).
- [15] S. Ono, H. C. Po, and H. Watanabe, Refined symmetry indicators for topological superconductors in all space groups, *Sci. Adv.* **6**, eaaz8367 (2020).
- [16] A. Alexandradinata, A. Nelson, and A. A. Soluyanov, Teleportation of Berry curvature on the surface of a Hopf insulator, *Phys. Rev. B* **103**, 045107 (2021).
- [17] A. Altland, P. W. Brouwer, J. Dieplinger, M. S. Foster, M. Moreno-Gonzalez, and L. Trifunovic, Fragility of Surface States in Non-Wigner-Dyson Topological Insulators, *Phys. Rev. X* **14**, 011057 (2024).
- [18] M. S. Rudner and L. S. Levitov, Topological Transition in a Non-Hermitian Quantum Walk, *Phys. Rev. Lett.* **102**, 065703 (2009).
- [19] M. Sato, K. Hasebe, K. Esaki, and M. Kohmoto, Time-Reversal Symmetry in Non-Hermitian Systems, *Prog. Theor. Phys.* **127**, 937 (2012); K. Esaki, M. Sato, K. Hasebe, and M. Kohmoto, Edge states and topological phases in non-Hermitian systems, *Phys. Rev. B* **84**, 205128 (2011).
- [20] Y. C. Hu and T. L. Hughes, Absence of topological insulator phases in non-Hermitian PT -symmetric Hamiltonians, *Phys. Rev. B* **84**, 153101 (2011).
- [21] H. Schomerus, Topologically protected midgap states in complex photonic lattices, *Opt. Lett.* **38**, 1912 (2013).
- [22] S. Longhi, D. Gatti, and G. D. Valle, Robust light transport in non-Hermitian photonic lattices, *Sci. Rep.* **5**, 13376 (2015).
- [23] T. E. Lee, Anomalous Edge State in a Non-Hermitian Lattice, *Phys. Rev. Lett.* **116**, 133903 (2016).
- [24] D. Leykam, K. Y. Bliokh, C. Huang, Y. D. Chong, and F. Nori, Edge Modes, Degeneracies, and Topological Numbers in Non-Hermitian Systems, *Phys. Rev. Lett.* **118**, 040401 (2017).
- [25] Y. Xu, S.-T. Wang, and L.-M. Duan, Weyl Exceptional Rings in a Three-Dimensional Dissipative Cold Atomic Gas, *Phys. Rev. Lett.* **118**, 045701 (2017).
- [26] H. Shen, B. Zhen, and L. Fu, Topological Band Theory for Non-Hermitian Hamiltonians, *Phys. Rev. Lett.* **120**, 146402 (2018); V. Kozii and L. Fu, Non-Hermitian topological theory of finite-lifetime quasiparticles: Prediction of bulk Fermi arc due to exceptional point, *Phys. Rev. B* **109**, 235139 (2024).
- [27] K. Takata and M. Notomi, Photonic Topological Insulating Phase Induced Solely by Gain and Loss, *Phys. Rev. Lett.* **121**, 213902 (2018).
- [28] V. M. Martinez Alvarez, J. E. Barrios Vargas, and L. E. F. Foa Torres, Non-Hermitian robust edge states in one dimension: Anomalous localization and eigenspace condensation at

- exceptional points, *Phys. Rev. B* **97**, 121401(R) (2018).
- [29] Z. Gong, Y. Ashida, K. Kawabata, K. Takasan, S. Higashikawa, and M. Ueda, Topological Phases of Non-Hermitian Systems, *Phys. Rev. X* **8**, 031079 (2018); K. Kawabata, S. Higashikawa, Z. Gong, Y. Ashida, and M. Ueda, Topological unification of time-reversal and particle-hole symmetries in non-Hermitian physics, *Nat. Commun.* **10**, 297 (2019).
- [30] S. Yao and Z. Wang, Edge States and Topological Invariants of Non-Hermitian Systems, *Phys. Rev. Lett.* **121**, 086803 (2018); S. Yao, F. Song, and Z. Wang, Non-Hermitian Chern Bands, *Phys. Rev. Lett.* **121**, 136802 (2018).
- [31] F. K. Kunst, E. Edvardsson, J. C. Budich, and E. J. Bergholtz, Biorthogonal Bulk-Boundary Correspondence in Non-Hermitian Systems, *Phys. Rev. Lett.* **121**, 026808 (2018).
- [32] A. McDonald, T. Pereg-Barnea, and A. A. Clerk, Phase-Dependent Chiral Transport and Effective Non-Hermitian Dynamics in a Bosonic Kitaev-Majorana Chain, *Phys. Rev. X* **8**, 041031 (2018).
- [33] C. H. Lee and R. Thomale, Anatomy of skin modes and topology in non-Hermitian systems, *Phys. Rev. B* **99**, 201103(R) (2019).
- [34] T. Liu, Y.-R. Zhang, Q. Ai, Z. Gong, K. Kawabata, M. Ueda, and F. Nori, Second-Order Topological Phases in Non-Hermitian Systems, *Phys. Rev. Lett.* **122**, 076801 (2019).
- [35] C. H. Lee, L. Li, and J. Gong, Hybrid Higher-Order Skin-Topological Modes in Nonreciprocal Systems, *Phys. Rev. Lett.* **123**, 016805 (2019).
- [36] K. Kawabata, K. Shiozaki, M. Ueda, and M. Sato, Symmetry and Topology in Non-Hermitian Physics, *Phys. Rev. X* **9**, 041015 (2019).
- [37] H. Zhou and J. Y. Lee, Periodic table for topological bands with non-Hermitian symmetries, *Phys. Rev. B* **99**, 235112 (2019).
- [38] L. Herviou, J. H. Bardarson, and N. Regnault, Defining a bulk-edge correspondence for non-Hermitian Hamiltonians via singular-value decomposition, *Phys. Rev. A* **99**, 052118 (2019).
- [39] H.-G. Zirnstein, G. Refael, and B. Rosenow, Bulk-Boundary Correspondence for Non-Hermitian Hamiltonians via Green Functions, *Phys. Rev. Lett.* **126**, 216407 (2021).
- [40] D. S. Borgnia, A. J. Kruchkov, and R.-J. Slager, Non-Hermitian Boundary Modes and Topology, *Phys. Rev. Lett.* **124**, 056802 (2020).
- [41] K. Kawabata, T. Bessho, and M. Sato, Classification of Exceptional Points and Non-Hermitian Topological Semimetals, *Phys. Rev. Lett.* **123**, 066405 (2019).
- [42] K. Yokomizo and S. Murakami, Non-Bloch Band Theory of Non-Hermitian Systems, *Phys. Rev. Lett.* **123**, 066404 (2019).
- [43] J. Y. Lee, J. Ahn, H. Zhou, and A. Vishwanath, Topological Correspondence between Hermitian and Non-Hermitian Systems: Anomalous Dynamics, *Phys. Rev. Lett.* **123**, 206404 (2019).
- [44] C. C. Wanjura, M. Brunelli, and A. Nunnenkamp, Topological framework for directional amplification in driven-dissipative cavity arrays, *Nat. Commun.* **11**, 3149 (2020).
- [45] K. Zhang, Z. Yang, and C. Fang, Correspondence between Winding Numbers and Skin Modes in Non-Hermitian Systems, *Phys. Rev. Lett.* **125**, 126402 (2020).
- [46] N. Okuma, K. Kawabata, K. Shiozaki, and M. Sato, Topological Origin of Non-Hermitian Skin Effects, *Phys. Rev. Lett.* **124**, 086801 (2020).
- [47] T. Bessho and M. Sato, Nielsen-Ninomiya Theorem with Bulk Topology: Duality in Floquet and Non-Hermitian Systems, *Phys. Rev. Lett.* **127**, 196404 (2021).
- [48] M. M. Denner, A. Skurativska, F. Schindler, M. H. Fischer, R. Thomale, T. Bzdušek, and T. Neupert, Exceptional topological insulators, *Nat. Commun.* **12**, 5681 (2021).
- [49] R. Okugawa, R. Takahashi, and K. Yokomizo, Second-order topological non-Hermitian skin effects, *Phys. Rev. B* **102**, 241202(R) (2020).
- [50] K. Kawabata, M. Sato, and K. Shiozaki, Higher-order non-Hermitian skin effect, *Phys. Rev. B* **102**, 205118 (2020).
- [51] K. Kawabata, K. Shiozaki, and S. Ryu, Topological Field Theory of Non-Hermitian Systems, *Phys. Rev. Lett.* **126**, 216405 (2021).
- [52] K. Zhang, Z. Yang, and C. Fang, Universal non-Hermitian skin effect in two and higher dimensions, *Nat. Commun.* **13**, 2496 (2022).
- [53] X.-Q. Sun, P. Zhu, and T. L. Hughes, Geometric Response and Disclination-Induced Skin Effects in Non-Hermitian Systems, *Phys. Rev. Lett.* **127**, 066401 (2021).
- [54] S. Franca, V. Könye, F. Hassler, J. van den Brink, and C. Fulga, Non-Hermitian Physics without Gain or Loss: The Skin Effect of Reflected Waves, *Phys. Rev. Lett.* **129**, 086601 (2022).
- [55] D. Nakamura, T. Bessho, and M. Sato, Bulk-Boundary Correspondence in Point-Gap Topological Phases, *Phys. Rev. Lett.* **132**, 136401 (2024).
- [56] H.-Y. Wang, F. Song, and Z. Wang, Amoeba Formulation of Non-Bloch Band Theory in Arbitrary Dimensions, *Phys. Rev. X* **14**, 021011 (2024).
- [57] Y. O. Nakai, N. Okuma, D. Nakamura, K. Shimomura, and M. Sato, Topological enhancement of nonnormality in non-Hermitian skin effects, *Phys. Rev. B* **109**, 144203 (2024).
- [58] X.-R. Ma, K. Cao, X.-R. Wang, Z. Wei, Q. Du, and S.-P. Kou, Non-Hermitian chiral skin effect, *Phys. Rev. Research* **6**, 013213 (2024).
- [59] F. Schindler, K. Gu, B. Lian, and K. Kawabata, Hermitian Bulk – Non-Hermitian Boundary Correspondence, *PRX Quantum* **4**, 030315 (2023).
- [60] D. Nakamura, K. Inaka, N. Okuma, and M. Sato, Universal Platform of Point-Gap Topological Phases from Topological Materials, *Phys. Rev. Lett.* **131**, 256602 (2023).
- [61] S. Hamanaka, T. Yoshida, and K. Kawabata, Non-Hermitian Topology in Hermitian Topological Matter, *arXiv:2405.10015*.
- [62] E. J. Bergholtz, J. C. Budich, and F. K. Kunst, Exceptional topology of non-Hermitian systems, *Rev. Mod. Phys.* **93**, 015005 (2021).
- [63] N. Okuma and M. Sato, Non-Hermitian Topological Phenomena: A Review, *Annu. Rev. Condens. Matter Phys.* **14**, 83 (2023).
- [64] V. V. Konotop, J. Yang, and D. A. Zezyulin, Nonlinear waves in \mathcal{PT} -symmetric systems, *Rev. Mod. Phys.* **88**, 035002 (2016).
- [65] R. El-Ganainy, K. G. Makris, M. Khajavikhan, Z. H. Muslimani, S. Rotter, and D. N. Christodoulides, Non-Hermitian physics and PT symmetry, *Nat. Phys.* **14**, 11 (2018).
- [66] C. Poli, M. Bellec, U. Kuhl, F. Mortessagne, and H. Schemm, Selective enhancement of topologically induced interface states in a dielectric resonator chain, *Nat. Commun.* **6**, 6710 (2015).
- [67] J. M. Zeuner, M. C. Rechtsman, Y. Plotnik, Y. Lumer, S. Nolte, M. S. Rudner, M. Segev, and A. Szameit, Observation of a Topological Transition in the Bulk of a Non-Hermitian System, *Phys. Rev. Lett.* **115**, 040402 (2015).
- [68] B. Zhen, C. W. Hsu, Y. Igarashi, L. Lu, I. Kaminer, A. Pick, S.-L. Chua, J. D. Joannopoulos, and M. Soljačić, Spawning rings of exceptional points out of Dirac cones, *Nature* **525**, 354

- (2015); H. Zhou, C. Peng, Y. Yoon, C. W. Hsu, K. A. Nelson, L. Fu, J. D. Joannopoulos, M. Soljačić, and B. Zhen, Observation of bulk Fermi arc and polarization half charge from paired exceptional points, *Science* **359**, 1009 (2018).
- [69] S. Weimann, M. Kremer, Y. Plotnik, Y. Lumer, S. Nolte, K. G. Makris, M. Segev, M. C. Rechtsman, and A. Szameit, Topologically protected bound states in photonic parity-time-symmetric crystals, *Nat. Mater.* **16**, 433 (2017).
- [70] L. Xiao, X. Zhan, Z. H. Bian, K. K. Wang, X. Zhang, X. P. Wang, J. Li, K. Mochizuki, D. Kim, N. Kawakami, W. Yi, H. Obuse, B. C. Sanders, and P. Xue, Observation of topological edge states in parity-time-symmetric quantum walks, *Nat. Phys.* **13**, 1117 (2017).
- [71] P. St-Jean, V. Goblot, E. Galopin, A. Lemaître, T. Ozawa, L. L. Gratiet, I. Sagnes, J. Bloch, and A. Amo, Lasing in topological edge states of a one-dimensional lattice, *Nat. Photon.* **11**, 651 (2017).
- [72] B. Bahari, A. Ndao, F. Vallini, A. E. Amili, Y. Fainman, and B. Kanté, Nonreciprocal lasing in topological cavities of arbitrary geometries, *Science* **358**, 636 (2017).
- [73] H. Zhao, P. Miao, M. H. Teimourpour, S. Malzard, R. El-Ganainy, H. Schomerus, and L. Feng, Topological hybrid silicon microlasers, *Nat. Commun.* **9**, 981 (2018).
- [74] M. A. Bandres, S. Wittek, G. Harari, M. Parto, J. Ren, M. Segev, D. Christodoulides, and M. Khajavikhan, Topological insulator laser: Experiments, *Science* **359**, eaar4005 (2018).
- [75] H. Zhao, X. Qiao, T. Wu, B. Midya, S. Longhi, and L. Feng, Non-Hermitian topological light steering, *Science* **365**, 1163 (2019).
- [76] A. Ghatak, M. Brandenbourger, J. van Wezel, and C. Coullais, Observation of non-Hermitian topology and its bulk-edge correspondence in an active mechanical metamaterial, *Proc. Natl. Acad. Sci. USA* **117**, 29561 (2020).
- [77] T. Helbig, T. Hofmann, S. Imhof, M. Abdelghany, T. Kiessling, L. W. Molenkamp, C. H. Lee, A. Szameit, M. Greiter, and R. Thomale, Generalized bulk-boundary correspondence in non-Hermitian topoelectrical circuits, *Nat. Phys.* **16**, 747 (2020).
- [78] L. Xiao, T. Deng, K. Wang, G. Zhu, Z. Wang, W. Yi, and P. Xue, Non-Hermitian bulk-boundary correspondence in quantum dynamics, *Nat. Phys.* **16**, 761 (2020).
- [79] S. Weidemann, M. Kremer, T. Helbig, T. Hofmann, A. Stegmaier, M. Greiter, R. Thomale, and A. Szameit, Topological funneling of light, *Science* **368**, 311 (2020).
- [80] W. Zhang, X. Ouyang, X. Huang, X. Wang, H. Zhang, Y. Yu, X. Chang, Y. Liu, D.-L. Deng, and L.-M. Duan, Observation of Non-Hermitian Topology with Nonunitary Dynamics of Solid-State Spins, *Phys. Rev. Lett.* **127**, 090501 (2021).
- [81] Q. Liang, D. Xie, Z. Dong, H. Li, H. Li, B. Gadway, W. Yi, and B. Yan, Dynamic Signatures of Non-Hermitian Skin Effect and Topology in Ultracold Atoms, *Phys. Rev. Lett.* **129**, 070401 (2022).
- [82] N. Hatano and D. R. Nelson, Localization Transitions in Non-Hermitian Quantum Mechanics, *Phys. Rev. Lett.* **77**, 570 (1996); Vortex pinning and non-Hermitian quantum mechanics, *Phys. Rev. B* **56**, 8651 (1997).
- [83] See the Supplemental Material for details on the detachment of topological boundary states, intrinsic non-Hermitian topology, and K -theory classification.
- [84] This Z_2 subsector structure due to chiral symmetry (or equivalently, pseudo-Hermiticity) is also clarified by the combination of right and left eigenstates; see Sec. VIB in Ref. [36].
- [85] K. Shiozaki (in preparation).
- [86] In the Altland-Zirnbauer[†] symmetry classes, all the extrinsic non-Hermitian topology reduces to imaginary-line-gap topology. In fact, if it were reducible to real-line-gap topology, topological boundary states could open a gap even around zero energy.
- [87] K. Nomura, M. Koshino, and S. Ryu, Topological Delocalization of Two-Dimensional Massless Dirac Fermions, *Phys. Rev. Lett.* **99**, 146806 (2007).
- [88] Even if the boundary Hamiltonians are infinite dimensional, the boundary projectors and concomitant topological invariants can be formulated with finite-dimensional Bloch states.
- [89] C. L. Kane and E. J. Mele, Quantum Spin Hall Effect in Graphene, *Phys. Rev. Lett.* **95**, 226801 (2005); Z_2 Topological Order and the Quantum Spin Hall Effect, *Phys. Rev. Lett.* **95**, 146802 (2005).
- [90] L. Fu and C. L. Kane, Time reversal polarization and a Z_2 adiabatic spin pump, *Phys. Rev. B* **74**, 195312 (2006).
- [91] X.-L. Qi, T. L. Hughes, and S.-C. Zhang, Topological field theory of time-reversal invariant insulators, *Phys. Rev. B* **78**, 195424 (2008).
- [92] J. C. Y. Teo and C. L. Kane, Topological defects and gapless modes in insulators and superconductors, *Phys. Rev. B* **82**, 115120 (2010).
- [93] M. Karoubi, *K-Theory: An Introduction* (Springer, Berlin, Heidelberg, 1978).
- [94] M. F. Atiyah and I. M. Singer, Index theory for skew-adjoint Fredholm operators, *Publications Mathématiques de l'Institut des Hautes Scientifiques* **37**, 5 (1969).
- [95] D. S. Freed and G. W. Moore, Twisted Equivariant Matter, *Ann. Henri Poincaré* **14**, 1927 (2013).
- [96] G. C. Thiang, On the K -Theoretic Classification of Topological Phases of Matter, *Ann. Henri Poincaré* **17**, 757 (2016).
- [97] K. Shiozaki, M. Sato, and K. Gomi, Topological crystalline materials: General formulation, module structure, and wallpaper groups, *Phys. Rev. B* **95**, 235425 (2017).
- [98] K. Gomi, Freed-Moore K -theory, [arXiv:1705.09134](https://arxiv.org/abs/1705.09134).
- [99] C.-K. Chiu, H. Yao, and S. Ryu, Classification of topological insulators and superconductors in the presence of reflection symmetry, *Phys. Rev. B* **88**, 075142 (2013).
- [100] T. Morimoto and A. Furusaki, Topological classification with additional symmetries from Clifford algebras, *Phys. Rev. B* **88**, 125129 (2013).
- [101] K. Shiozaki and M. Sato, Topology of crystalline insulators and superconductors, *Phys. Rev. B* **90**, 165114 (2014).
- [102] J. Langbehn, Y. Peng, L. Trifunovic, F. von Oppen, and P. W. Brouwer, Reflection-Symmetric Second-Order Topological Insulators and Superconductors, *Phys. Rev. Lett.* **119**, 246401 (2017).
- [103] J. E. Moore, Y. Ran, and X.-G. Wen, Topological Surface States in Three-Dimensional Magnetic Insulators, *Phys. Rev. Lett.* **101**, 186805 (2008).
- [104] C. Fang and L. Fu, New classes of three-dimensional topological crystalline insulators: Nonsymmorphic and magnetic, *Phys. Rev. B* **91**, 161105 (2015).
- [105] K. Shiozaki, M. Sato, and K. Gomi, Z_2 topology in nonsymmorphic crystalline insulators: Möbius twist in surface states, *Phys. Rev. B* **91**, 155120 (2015); Topology of nonsymmorphic crystalline insulators and superconductors, *Phys. Rev. B* **93**, 195413 (2016).
- [106] B. Lapierre, L. Trifunovic, T. Neupert, and P. W. Brouwer, Topology of ultra-localized insulators and superconductors, [arXiv:2407.07957](https://arxiv.org/abs/2407.07957).

Supplemental Material for “Non-Hermitian Origin of Wannier Localizability and Detachable Topological Boundary States”

I. DETACHMENT OF TOPOLOGICAL BOUNDARY STATES

A. 2D class A

We consider a one-dimensional Dirac model

$$H(k_x) = k_x, \quad (\text{I.1})$$

for a chiral edge state of a two-dimensional topological insulator without symmetry (i.e., class A). An important feature of this Dirac model is a spectral flow. To see this, we couple it with a trivial band $H = 0$,

$$H(k_x) = \begin{pmatrix} k_x & v \\ v^* & 0 \end{pmatrix}, \quad (\text{I.2})$$

with the coupling amplitude $v \in \mathbb{C}$. The spectrum of this two-band model is obtained as

$$E(k_x) = \frac{k_x}{2} \pm \sqrt{\left(\frac{k_x}{2}\right)^2 + |v|^2}, \quad (\text{I.3})$$

which behaves

$$E(k_x) \rightarrow k_x, -\frac{|v|^2}{k_x} \quad (k \rightarrow \pm\infty). \quad (\text{I.4})$$

Thus, such a perturbation cannot open a spectral gap, implying the inevitable presence of the spectral flow.

B. 2D class AII

We consider a one-dimensional Dirac model

$$H(k_x) = k_x \sigma_x, \quad (\text{I.5})$$

which respects time-reversal symmetry

$$\sigma_y H^*(k_x) \sigma_y^{-1} = H(-k_x). \quad (\text{I.6})$$

Similarly to class A, this Dirac model exhibits a spectral flow. To see this, we again couple it with a trivial band $H = \varepsilon$ so that time-reversal symmetry will be respected,

$$H(k_x) = \begin{pmatrix} k_x \sigma_x & -iv \sigma_x \\ iv \sigma_x & \varepsilon \end{pmatrix} = \frac{1}{2} (k_x \sigma_x + \varepsilon) + \frac{1}{2} (k_x \sigma_x - \varepsilon) \tau_z + v \sigma_x \tau_y, \quad (\text{I.7})$$

with the coupling amplitude $v \in \mathbb{C}$. Since this four-band model commutes with σ_x , it consists of two independent two-band models in class A,

$$\begin{pmatrix} k_x & -iv \\ iv & \varepsilon \end{pmatrix}, \quad \begin{pmatrix} -k_x & iv \\ -iv & \varepsilon \end{pmatrix}, \quad (\text{I.8})$$

each of which exhibits a spectral flow, as discussed in Sec. IA.

The unitary symmetry that commutes with the Hamiltonian is specific to the above model and not necessarily present in generic models. Nevertheless, the Dirac model generally accompanies a spectral flow as long as time-reversal symmetry in Eq. (I.6) is respected [87]. Let us put this Dirac model on a one-dimensional space with length L_x and under the twisted boundary conditions. For the twist angle ϕ , momentum k_x is quantized by

$$e^{ik_x L_x} = e^{i\phi}, \quad \text{i.e.,} \quad k_x L_x = \phi + 2n\pi \quad (n \in \mathbb{Z}), \quad (\text{I.9})$$

and hence the energy spectrum of the Dirac model in Eq. (I.5) is obtained as

$$E(\phi) = \pm \frac{\phi + 2n\pi}{L_x}. \quad (\text{I.10})$$

An important consequence of time-reversal symmetry in Eq. (I.6) is the Kramers degeneracy for $\phi \in \pi\mathbb{Z}$. On the other hand, for $\phi \notin \pi\mathbb{Z}$, time-reversal symmetry is broken, resulting in no Kramers degeneracy. Through the adiabatic change of the flux ϕ , each of the original Kramers pairs for $\phi = 0$ splits for $0 < \phi < \pi$ and then meets the other half of the other Kramers pairs. Such switches of the Kramers pairs inevitably require the energy cutoff in high energy and the concomitant spectral flow. It is notable that this discussion is also applicable to two-dimensional and three-dimensional Dirac models with time-reversal symmetry in Eq. (I.6). Additionally, it is applicable even in the presence of disorder that breaks translation invariance.

C. 3D class AIII

We consider a two-dimensional Dirac model

$$H(k_x, k_y) = k_x \sigma_x + k_y \sigma_y, \quad (\text{I.11})$$

which respects chiral symmetry

$$\sigma_z H(k_x, k_y) \sigma_z^{-1} = -H(k_x, k_y). \quad (\text{I.12})$$

This continuum model describes a surface state of a three-dimensional topological insulator in class AIII. Notably, this chiral-symmetric Dirac model exhibits no spectral flow [17]. To confirm this, we couple it to a trivial band and study the four-band model,

$$\begin{aligned} H(k_x, k_y) &= \begin{pmatrix} k_x \sigma_x + k_y \sigma_y & v \sigma_- \\ v \sigma_+ & \varepsilon \sigma_x \end{pmatrix} \\ &= \frac{1}{2} ((k_x + \varepsilon) \sigma_x + k_y \sigma_y) + \frac{1}{2} ((k_x - \varepsilon) \sigma_x + k_y \sigma_y) \tau_z + \frac{v}{2} (\sigma_x \tau_x + \sigma_y \tau_y), \end{aligned} \quad (\text{I.13})$$

where $\varepsilon \sigma_x$ ($\varepsilon \geq 0$) is a trivial band, and $v \geq 0$ denotes the coupling strength to the Dirac model. The entire four-band model remains to respect chiral symmetry in Eq. (I.12). Since we have

$$2H^2(k_x, k_y) = k_x^2 + k_y^2 + \varepsilon^2 + v^2 + v(k_x + \varepsilon + (k_x - \varepsilon)\sigma_z)\tau_x + vk_y(1 + \sigma_z)\tau_y + (k_x^2 + k_y^2 - \varepsilon^2 - v^2\sigma_z)\tau_z, \quad (\text{I.14})$$

H^2 commutes with σ_z .

- For $\sigma_z = +1$, we have

$$2H^2(k_x, k_y) = k_x^2 + k_y^2 + \varepsilon^2 + v^2 + 2vk_x\tau_x + 2vk_y\tau_y + (k_x^2 + k_y^2 - \varepsilon^2 - v^2)\tau_z, \quad (\text{I.15})$$

and hence the energy bands are determined by

$$\begin{aligned} 2E^2(k_x, k_y) &= k^2 + \varepsilon^2 + v^2 \pm \sqrt{(k^2 - \varepsilon^2 - v^2)^2 + 4v^2k^2} \\ &= k^2 + \varepsilon^2 + v^2 \pm \sqrt{(k^2 - \varepsilon^2 + v^2)^2 + 4\varepsilon^2v^2} \end{aligned} \quad (\text{I.16})$$

with $k^2 := k_x^2 + k_y^2$.

- For $\sigma_z = -1$, we have

$$2H^2(k_x, k_y) = k_x^2 + k_y^2 + \varepsilon^2 + v^2 + 2\varepsilon v\tau_x + (k_x^2 + k_y^2 - \varepsilon^2 + v^2)\tau_z, \quad (\text{I.17})$$

and hence the energy bands are again determined by Eq. (I.16).

Therefore, regardless of σ_z , the four energy bands are obtained as

$$\sqrt{2}E(k) = \pm \sqrt{k^2 + \varepsilon^2 + v^2 \pm \sqrt{(k^2 - \varepsilon^2 + v^2)^2 + 4\varepsilon^2v^2}}. \quad (\text{I.18})$$

Around the Dirac point (i.e., $|k_x|, |k_y| \ll \varepsilon, v$), we have

$$E(k) = \pm \sqrt{\varepsilon^2 + v^2} + O(k^2), \pm \frac{\varepsilon}{\sqrt{\varepsilon^2 + v^2}} k + O(k^3). \quad (\text{I.19})$$

In the ultraviolet limit (i.e., $|k_x|, |k_y| \rightarrow \infty$), on the other hand, we have

$$E(k) = \pm \sqrt{k^2 + v^2} + O(1/k^2), \pm \varepsilon + O(1/k^2). \quad (\text{I.20})$$

Thus, the four-band model exhibits a global gap

$$\Delta = \sqrt{\varepsilon^2 + v^2} - \varepsilon. \quad (\text{I.21})$$

II. A MODEL OF DETACHED AND FLAT-BAND SURFACE STATE

We present a Hermitian lattice model with a flat and detached surface state for three dimensions $d = 3$ in class AIII. The construction here can be straightforwardly generalized to any odd spatial dimension $d = 2n + 1$ with the even winding numbers $W_{2n+1} \in 2\mathbb{Z}$. Consider the following four-band model in class AIII:

$$H(\mathbf{h}(k_x, k_y), k_z) = (\cos k_z) \tau_x \otimes \sigma_0 + (\sin k_z) \tau_y \otimes \mathbf{h}(k_x, k_y) \cdot \boldsymbol{\sigma}, \quad (\text{II.1})$$

$$\mathbf{h}(k_x, k_y) = (\sin k_x, \sin k_y, m - \cos k_x - \cos k_y), \quad (\text{II.2})$$

satisfying chiral symmetry

$$\Gamma H(\mathbf{h}(k_x, k_y), k_z) \Gamma^{-1} = -H(\mathbf{h}(k_x, k_y), k_z), \quad \Gamma = \tau_z. \quad (\text{II.3})$$

By writing the Hamiltonian as

$$H(\mathbf{h}(k_x, k_y), k_z) = \begin{pmatrix} & q^\dagger(\mathbf{k}) \\ q(\mathbf{k}) & \end{pmatrix} \quad \text{with} \quad q(\mathbf{k}) = \cos k_z + i(\sin k_z) \mathbf{h}(k_x, k_y) \cdot \boldsymbol{\sigma}, \quad (\text{II.4})$$

the three-dimensional winding number is obtained as

$$W_3 = \frac{1}{24\pi^2} \int_{T^3} \text{tr} [q^{-1} dq]^3 = \begin{cases} 0 & (|m| > 2); \\ -2 & (0 < m < 2); \\ 2 & (-2 < m < 0). \end{cases} \quad (\text{II.5})$$

This reflects twice the Chern number of the Hamiltonian $\mathbf{h}(\mathbf{k}) \cdot \boldsymbol{\sigma}$ for two dimensions $d = 2$ and class A.

Viewing \mathbf{h} as a parameter, we consider the following one-dimensional lattice model along the z direction:

$$\hat{H}_{1D}(\mathbf{h}) = \sum_{z \in \mathbb{Z}} \psi_{z+1}^\dagger \frac{\tau_x + i\tau_y \mathbf{h} \cdot \boldsymbol{\sigma}}{2} \psi_z + \text{H.c.}, \quad (\text{II.6})$$

where ψ_z is the four-component complex fermion operator at site z . For the semi-infinite boundary conditions where $z \leq 0$ is in the topological insulator and $z > 0$ is in the vacuum, for every $|\mathbf{h}| > 0$, the interface $z = 0$ hosts two exponentially localized zero-energy states, given as

$$\phi_+(z, \mathbf{h}) = u_+(\hat{h}) \otimes \begin{pmatrix} 0 \\ \eta_-(z; h) \end{pmatrix}_\tau, \quad \phi_-(z, \mathbf{h}) = u_-(\hat{h}) \otimes \begin{pmatrix} \eta_+(z; h) \\ 0 \end{pmatrix}_\tau, \quad (\text{II.7})$$

with $h = |\mathbf{h}|$ and $\hat{h} = \mathbf{h}/|\mathbf{h}|$. Here, $u_\pm(\hat{h}) \in \mathbb{C}^2$ is a normalized two-component vector in the σ space, satisfying $(\mathbf{h} \cdot \boldsymbol{\sigma}) u_\pm(\hat{h}) = \pm h u_\pm(\hat{h})$, and $(0, \eta_-(z; h))_\tau^T$ and $(\eta_+(z; h), 0)_\tau^T$ are respectively normalized vectors in the τ and z space whose localization lengths depend on h . Note that $\phi_+(z, \mathbf{h})$ and $\phi_-(z, \mathbf{h})$ have chirality $\Gamma = 1$ and $\Gamma = -1$, respectively. Using the polar coordinates of \hat{h} as in $\hat{h} = (\theta_h, \phi_h)$, $u_\pm(\hat{h})$ is explicitly given, up to a $U(1)$ phase, as

$$u_+(\hat{h}) \propto \begin{pmatrix} \cos \frac{\theta_h}{2} \\ e^{i\phi_h} \sin \frac{\theta_h}{2} \end{pmatrix}_\sigma, \quad u_-(\hat{h}) \propto \begin{pmatrix} -e^{-i\phi_h} \sin \frac{\theta_h}{2} \\ \cos \frac{\theta_h}{2} \end{pmatrix}_\sigma. \quad (\text{II.8})$$

Thus, we get the two-component flat detached surface state, irrespective of the winding number W_3 .

Now, consider a generic perturbation to this flat-band surface state. The effective 2×2 Hamiltonian with a chiral-symmetry-preserving perturbation $H_V(\mathbf{h})$ is

$$H_{\text{eff}}(\mathbf{h}) = \int dz (\phi_+(z, \mathbf{h}), \phi_-(z, \mathbf{h}))^\dagger H_V(\mathbf{h}) (\phi_+(z, \mathbf{h}), \phi_-(z, \mathbf{h})). \quad (\text{II.9})$$

Notably, while $H_V(\mathbf{h})$ is gauge-independent, $\phi_\pm(z, \mathbf{h})$'s are gauge-dependent, and thus the effective Hamiltonian $H_{\text{eff}}(\mathbf{h})$ is also gauge-dependent. Express $H_V(\mathbf{h})$ in the τ space as

$$H_V(\mathbf{h}) = \begin{pmatrix} & V^\dagger(\mathbf{h}) \\ V(\mathbf{h}) & \end{pmatrix}_\tau, \quad (\text{II.10})$$

and introduce the 2×2 matrix

$$v(\mathbf{h}) = \int dz \eta_-(z; \mathbf{h})^* V(\mathbf{h}) \eta_+(z; \mathbf{h}), \quad (\text{II.11})$$

then the effective Hamiltonian becomes

$$H_{\text{eff}}(\mathbf{h}) = \begin{pmatrix} & u_+^\dagger(\hat{h})v^\dagger(\mathbf{h})u_-(\hat{h}) \\ u_-^\dagger(\hat{h})v(\mathbf{h})u_+(\hat{h}) & \end{pmatrix}. \quad (\text{II.12})$$

Thus, the spectrum of the surface states is

$$\pm |z(\mathbf{h})|, \quad z(\mathbf{h}) = u_-^\dagger(\hat{h})v(\mathbf{h})u_+(\hat{h}) \in \mathbb{C}. \quad (\text{II.13})$$

Note that the absolute value $|z(\mathbf{h})|$ is gauge-invariant. We show that there is no perturbation $v(\mathbf{h})$ such that $|z(\mathbf{h})| > 0$ for all $\hat{h} \in S^2$, as follows.

Proof.—We rewrite $|z|^2$ in the following manner,

$$|z|^2 = \text{tr} [vu_+u_+^\dagger v^\dagger u_-u_-^\dagger] = \text{tr} \left[v \frac{1 + \hat{h} \cdot \boldsymbol{\sigma}}{2} v^\dagger \frac{1 - \hat{h} \cdot \boldsymbol{\sigma}}{2} \right] = \frac{1}{4} \text{tr} [vv^\dagger + (v^\dagger v - vv^\dagger)\hat{h} \cdot \boldsymbol{\sigma} - v\hat{h} \cdot \boldsymbol{\sigma}v^\dagger \hat{h} \cdot \boldsymbol{\sigma}]. \quad (\text{II.14})$$

Using $v = v_0 + \mathbf{v} \cdot \boldsymbol{\sigma}$, we have from straightforward calculations

$$|z|^2 = (\hat{h} \times \mathbf{v}) \cdot (\hat{h} \times \mathbf{v}^*) - i\hat{h} \cdot (\mathbf{v}^* \times \mathbf{v}). \quad (\text{II.15})$$

We decompose \mathbf{v} into the component of the polar coordinate $\mathbf{v} = v_h \hat{h} + v_\theta \hat{\theta} + v_\phi \hat{\phi}$ and get

$$|z|^2 = |v_\theta - iv_\phi|^2. \quad (\text{II.16})$$

Further separating \mathbf{v} into real and imaginary parts $\mathbf{v} = \mathbf{v}_1 + i\mathbf{v}_2$ leads to

$$|z|^2 = (v_{1\theta} + v_{2\phi})^2 + (v_{2\theta} - v_{1\phi})^2. \quad (\text{II.17})$$

Introducing vectors on the tangent space TS^2 ,

$$\mathbf{v}_1^\perp = \mathbf{v}_1 - (\hat{h} \cdot \mathbf{v}_1)\hat{h}, \quad \mathbf{v}_2^\perp = \mathbf{v}_2 - (\hat{h} \cdot \mathbf{v}_2)\hat{h}, \quad (\text{II.18})$$

we eventually get the following form:

$$|z|^2 = |\mathbf{v}_1^\perp - \hat{h} \times \mathbf{v}_2^\perp|^2. \quad (\text{II.19})$$

The vector $\mathbf{v}_1^\perp - \hat{h} \times \mathbf{v}_2^\perp$ is in the tangent space TS^2 . According to the Poincaré-Hopf theorem, there must be two defects on S^2 where the tangent vector $\mathbf{v}_1^\perp - \hat{h} \times \mathbf{v}_2^\perp$ vanishes. \square

Alternative proof.—Note that $u_+(\hat{h})$ and $u_-(\hat{h})$ are orthonormal bases of \mathbb{C}^2 . The 2×2 matrix $v(\mathbf{h})$ is expanded locally in S^2 as

$$v(\mathbf{h}) = \sum_{i,j \in \{+,-\}} v_{ij}(\mathbf{h}) u_i(\hat{h}) u_j^\dagger(\hat{h}), \quad v_{ij}(\mathbf{h}) = u_i^\dagger(\hat{h}) v(\mathbf{h}) u_j(\hat{h}), \quad (\text{II.20})$$

so that $z(\mathbf{h}) = v_{-+}(\mathbf{h})$. Note that

$$u_i(\hat{h})u_j^\dagger(\hat{h}) \in \text{Mat}_{2 \times 2}(\mathbb{C}) \cong \mathbb{C}^2 \otimes (\mathbb{C}^2)^* \quad (\text{II.21})$$

defines a line bundle over S^2 with the fiber space $\text{Mat}_{2 \times 2}(\mathbb{C})$. The line bundle defined by $u_-(\hat{h})u_+^\dagger(\hat{h})$ has the Chern number of 2. Assuming $v_{-+}(\mathbf{h}) \neq 0$ everywhere on S^2 means that there exists a global section of the nontrivial line bundle $u_-(\hat{h})u_+^\dagger(\hat{h})$, leading to a contradiction. \square

A consequence of this statement is that if the detached surface state acquires a uniform mass gap in the whole surface Brillouin zone $(k_x, k_y) \in T^2$, the degree of the map $\hat{h} : T^2 \rightarrow S^2$, which coincides with the Chern number of the two-dimensional Hamiltonian $\mathbf{h}(k_x, k_y) \cdot \boldsymbol{\sigma}$ in class A and thus the winding number W_3 of the three-dimensional bulk, must be trivial.

III. FROM POINT GAP TO IMAGINARY LINE GAP

We provide a one-parameter point-gapped model in two dimensions for class AIII that shows imaginary-line-gap opening while retaining a point gap:

$$H_\theta(k_x, k_y) := \Gamma U(\theta) \Gamma h(k_x, k_y) U^\dagger(\theta) - i\sigma_0 \tau_0 \quad (\Gamma := \sigma_z \tau_0), \quad (\text{III.1})$$

with a one parameter $\theta \in [0, 1]$ and

$$U(\theta) := \exp\left[\frac{i\pi\theta}{4}\sigma_y(\tau_0 + \tau_z)\right] \exp\left[\frac{i\pi\theta}{4}(\sigma_0 + \sigma_z)\tau_y\right], \quad (\text{III.2})$$

$$h(k_x, k_y) := \frac{1}{\mathcal{N}} [\sin k_x \sigma_x + (1 - \cos k_x - \cos k_y) \sigma_y + i \sin k_y \sigma_0] \frac{\tau_0 + \tau_z}{2} + i\sigma_0 \frac{\tau_0 - \tau_z}{2}, \quad (\text{III.3})$$

$$\mathcal{N} := \sqrt{\sin^2 k_x + (1 - \cos k_x - \cos k_y)^2 + \sin^2 k_y}. \quad (\text{III.4})$$

For arbitrary $\theta \in [0, 1]$, this model indeed respects chiral symmetry:

$$\Gamma H_\theta^\dagger \Gamma^{-1} = -H_\theta. \quad (\text{III.5})$$

For $\theta = 0$, this model reduces to

$$H_0(k_x, k_y) = \frac{1}{\mathcal{N}} [\sin k_x \sigma_x + (1 - \cos k_x - \cos k_y) \sigma_y + i(\sin k_y - \mathcal{N})\sigma_0] \frac{\tau_0 + \tau_z}{2}, \quad (\text{III.6})$$

which is nothing but Eq. (4) in the main text with $\gamma = 1$, up to normalization and stacking with trivial bands. H_0 has a point gap around $E_P = -i$ and exhibits nontrivial point-gap topology (i.e., $\text{Ch}_1[i(H_0 - E_P)\Gamma] \neq 0$), as explained in the main text. Since Γ and $U(\theta)$ are unitary matrices, it is straightforward to confirm that H_θ keeps the point gap at E_P and chiral symmetry even for arbitrary $0 < \theta \leq 1$.

As illustrated in Fig. S1, with increasing θ , eigenstates with $\text{Im}E < 0$ leave from those with $E = 0$, leading to opening of an imaginary line gap with respect to $E_L = -1$. Finally, H_θ reaches an anti-Hermitian Chern insulator at $\theta = 1$ while keeping the point gap at E_P :

$$H_1(k_x, k_y) = \frac{\sigma_0 + \sigma_z}{2} \frac{i}{\mathcal{N}} [\sin k_x \tau_y + (1 - \cos k_x - \cos k_y) \tau_x - \sin k_y \tau_z] - \frac{\sigma_0 - \sigma_z}{2} i\tau_z - i\sigma_0 \tau_0. \quad (\text{III.7})$$

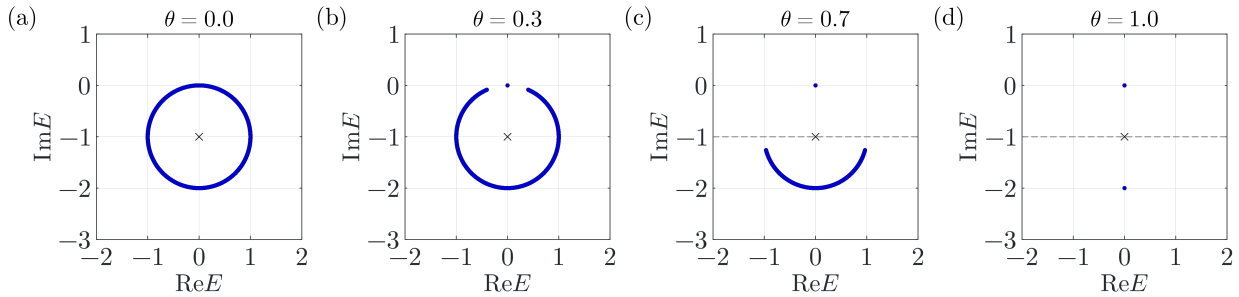


FIG. S1. Opening of an imaginary line gap while keeping a point gap. The complex spectrum of the point-gapped two-dimensional model $H_\theta(k_x, k_y)$ in class AIII [Eq. (III.1)] is shown for (a) $\theta = 0.0$, (b) $\theta = 0.3$, (c) $\theta = 0.7$, and (d) $\theta = 1.0$.

IV. BULK-BOUNDARY CORRESPONDENCE

Our classification also uncovers the topological nature of the detached boundary states. For a gapped d -dimensional Hermitian Hamiltonian $H(\mathbf{k})$, the bulk topological invariant is defined [4, 6]. For the semi-infinite boundary conditions with a boundary perpendicular to the x_d direction, the boundary Hamiltonian $\hat{H}(\mathbf{k}_{\parallel})$ is defined, where $\mathbf{k}_{\parallel} = (k_1, \dots, k_{d-1})$ is the Bloch momentum for the surface Brillouin zone. Note that the matrix size of $\hat{H}(\mathbf{k}_{\parallel})$ is infinite due to the bulk degrees of freedom. Suppose that the boundary Hamiltonian $\hat{H}(\mathbf{k}_{\parallel})$ hosts states detached from the bulk spectrum; the orthogonal projection onto the detached states is defined as

$$\hat{P}(\mathbf{k}_{\parallel}) = \frac{1}{2\pi i} \oint_C \frac{dz}{z - \hat{H}(\mathbf{k}_{\parallel})}, \quad (\text{IV.1})$$

where C is a symmetry-preserving loop in the complex energy plane surrounding the spectrum of the detached states (see Fig. S2). $\hat{P}(\mathbf{k}_{\parallel})$ sends the bulk state to 0 and the detached boundary states to 1. Notably, particle-hole and chiral symmetries behave as time-reversal and \mathbb{Z}_2 symmetries, respectively, within the sub-Hilbert space of the detached boundary states:

$$\hat{C}\hat{P}^*(\mathbf{k}_{\parallel})\hat{C}^{-1} = \hat{P}(-\mathbf{k}_{\parallel}) \quad (\hat{C}\hat{C}^* = \pm 1), \quad (\text{IV.2})$$

$$\hat{\Gamma}\hat{P}(\mathbf{k}_{\parallel})\hat{\Gamma}^{-1} = \hat{P}(\mathbf{k}_{\parallel}) \quad (\text{IV.3})$$

with unitary operators \hat{C} and $\hat{\Gamma}$ for particle-hole and chiral symmetries. Accordingly, we define the $(d-1)$ -dimensional topological invariants for the detached boundary states protected by \hat{C} and $\hat{\Gamma}$, as specified below.

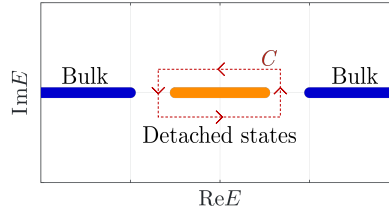


FIG. S2. Projection onto the detached boundary states. The loop C is chosen to respect symmetry and enclose the spectrum of the detached boundary states in the complex energy plane.

For odd $d = 2n + 1$ in the presence of chiral symmetry, using the projector $\hat{P}^{(\pm)}(\mathbf{k}_{\parallel}) := \hat{P}(\mathbf{k}_{\parallel})(1 \pm \hat{\Gamma})/2$ for each chirality $\hat{\Gamma} = \pm 1$, two independent Chern numbers are defined as

$$\text{Ch}_n \left[\hat{P}^{(\pm)}(\mathbf{k}_{\parallel}) \right] := \frac{1}{n!} \left(\frac{i}{2\pi} \right)^n \int_{T^{d-1}} \text{Tr} \left[\left(\hat{P}^{(\pm)}(\mathbf{k}_{\parallel}) d\hat{P}^{(\pm)}(\mathbf{k}_{\parallel}) d\hat{P}^{(\pm)}(\mathbf{k}_{\parallel}) \right)^n \right]. \quad (\text{IV.4})$$

In the presence of particle-hole symmetry, as \hat{C} behaves as time-reversal symmetry, one can define \mathbb{Z}_2 invariants for the detached boundary states. Specifically, one can define the class-AII-type \mathbb{Z}_2 invariant $\nu_{\text{class AII}}^{d-1} \left[\hat{P}(\mathbf{k}_{\parallel}) \right]$ for class C in the boundary dimensions $d-1 = 8n+2, 8n+3$, and the class-AI-type \mathbb{Z}_2 invariant $\nu_{\text{class AI}}^{d-1} \left[\hat{P}(\mathbf{k}_{\parallel}) \right]$ for class D for $d-1 = 8n+6, 8n+7$ [4, 91, 92]. Furthermore, since particle-hole symmetry \hat{C} does not change the chirality (i.e., $\hat{C}\hat{\Gamma}^* = \hat{\Gamma}\hat{C}$) for classes CII and BDI, the class-AII-type \mathbb{Z}_2 invariant $\nu_{\text{class AII}}^{d-1} \left[\hat{P}^{(\pm)}(\mathbf{k}_{\parallel}) \right]$ for each sector $\hat{\Gamma} = \pm$ is well defined for class CII when $d-1 = 8n+2, 8n+3$. Similarly, the class-AI-type \mathbb{Z}_2 invariant $\nu_{\text{class AI}}^{d-1} \left[\hat{P}^{(\pm)}(\mathbf{k}_{\parallel}) \right]$ for each sector $\hat{\Gamma} = \pm$ is well defined for class BDI when $d-1 = 8n+6, 8n+7$.

The imaginary-line-gap to point-gap map described in Sec. V gives the relationship between the bulk and boundary invariants, summarized as follows. In the presence of chiral symmetry, we have

$$\text{Ch}_n \left[\hat{P}^{(+)}(\mathbf{k}_{\parallel}) \right] - \text{Ch}_n \left[\hat{P}^{(-)}(\mathbf{k}_{\parallel}) \right] = W_{2n+1} [H(\mathbf{k})], \quad (\text{IV.5})$$

where $W_{2n+1} [H(\mathbf{k})]$ is the $(2n+1)$ -dimensional winding number defined by the chiral-symmetric Hamiltonian $H(\mathbf{k})$. For classes DIII and CI, since particle-hole symmetry flips chirality as $\hat{C}\hat{\Gamma}^* = -\hat{\Gamma}\hat{C}$, we have $\text{Ch}_n \left[\hat{P}^{(+)}(\mathbf{k}_{\parallel}) \right] = -\text{Ch}_n \left[\hat{P}^{(-)}(\mathbf{k}_{\parallel}) \right]$,

meaning that if the boundary states are detached, the bulk winding number $W_{2n+1}[H(\mathbf{k})]$ should be even. This accounts for the “ $\mathbb{Z}^{\checkmark}/\times$ classification” in Table I. For the \mathbb{Z}_2 topological phases in the d -dimensional bulk, we obtain

$$\text{Ch}_{4n}[\hat{P}(\mathbf{k}_{\parallel})] \equiv \nu_{\text{class D}}^{d=8n+1}[H(\mathbf{k})] \pmod{2}, \quad (\text{IV.6})$$

$$\frac{1}{2}\text{Ch}_{4n}[\hat{P}(\mathbf{k}_{\parallel})] \equiv \nu_{\text{class DIII}}^{d=8n+1}[H(\mathbf{k})] \pmod{2}, \quad (\text{IV.7})$$

$$\nu_{\text{class AII}}^{d-1=8n+2}[\hat{P}^{(+)}(\mathbf{k}_{\parallel})] + \nu_{\text{class AII}}^{d-1=8n+2}[\hat{P}^{(-)}(\mathbf{k}_{\parallel})] = \nu_{\text{class CII}}^{d=8n+3}[H(\mathbf{k})], \quad (\text{IV.8})$$

$$\nu_{\text{class AII}}^{d-1=8n+3}[\hat{P}^{(+)}(\mathbf{k}_{\parallel})] + \nu_{\text{class AII}}^{d-1=8n+3}[\hat{P}^{(-)}(\mathbf{k}_{\parallel})] = \nu_{\text{class CII}}^{d=8n+4}[H(\mathbf{k})], \quad (\text{IV.9})$$

$$\nu_{\text{class AII}}^{d-1=8n+3}[\hat{P}(\mathbf{k}_{\parallel})] = \nu_{\text{class C}}^{d=8n+4}[H(\mathbf{k})], \quad (\text{IV.10})$$

$$\text{Ch}_{4n+2}[\hat{P}(\mathbf{k}_{\parallel})] \equiv \nu_{\text{class C}}^{d=8n+5}[H(\mathbf{k})] \pmod{2}, \quad (\text{IV.11})$$

$$\frac{1}{2}\text{Ch}_{4n+2}[\hat{P}(\mathbf{k}_{\parallel})] \equiv \nu_{\text{class CI}}^{d=8n+5}[H(\mathbf{k})] \pmod{2}, \quad (\text{IV.12})$$

$$\nu_{\text{class AI}}^{d-1=8n+6}[\hat{P}^{(+)}(\mathbf{k}_{\parallel})] + \nu_{\text{class AI}}^{d-1=8n+6}[\hat{P}^{(-)}(\mathbf{k}_{\parallel})] = \nu_{\text{class BDI}}^{d=8n+7}[H(\mathbf{k})], \quad (\text{IV.13})$$

$$\nu_{\text{class AI}}^{d-1=8n+7}[\hat{P}^{(+)}(\mathbf{k}_{\parallel})] + \nu_{\text{class AI}}^{d-1=8n+7}[\hat{P}^{(-)}(\mathbf{k}_{\parallel})] = \nu_{\text{class BDI}}^{d=8n+8}[H(\mathbf{k})], \quad (\text{IV.14})$$

$$\nu_{\text{class AI}}^{d-1=8n+7}[\hat{P}(\mathbf{k}_{\parallel})] = \nu_{\text{class D}}^{d=8n+8}[H(\mathbf{k})]. \quad (\text{IV.15})$$

Here, the zeroth Chern number $\text{Ch}_0[\hat{P}]$ is the rank of \hat{P} . These formulas (IV.5)-(IV.15) clarify the topology of the detached boundary states, leading to unique boundary responses and disorder effects.

Meanwhile, the stability of the detached boundary states is ensured by real-line-gap (or equivalently, Hermitian) topology [47]. In fact, if a real line gap were open, point-gap topology could be trivialized by continuously moving the reference point far away, which would contradict the stability of point-gap topology (see Fig. S3). Consistently, all the extrinsic non-Hermitian topology reduces to imaginary-line-gap topology, as summarized in Table S1.

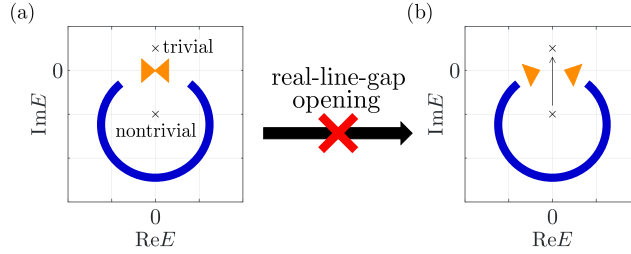


FIG. S3. Prohibition against real-line-gap opening due to nontrivial point-gap topology.

V. INTRINSIC NON-HERMITIAN TOPOLOGY

We develop the classification of intrinsic non-Hermitian topology, as shown in Table S1 (see also Sec. SIX in the Supplemental Material of Ref. [46], as well as Ref. [85]). As also discussed in the main text, if a line gap is open, a point gap is also open for a reference point on the reference line. Thus, we can introduce a map from line-gapped topological phases to point-gapped topological phases for each spatial dimension and symmetry class. Given a d -dimensional non-Hermitian Hamiltonian $H(\mathbf{k})$, we consider the Hermitized Hamiltonian

$$\tilde{H}(\mathbf{k}) := \begin{pmatrix} 0 & H(\mathbf{k}) \\ H^\dagger(\mathbf{k}) & 0 \end{pmatrix}_\sigma, \quad (\text{V.1})$$

which respects chiral symmetry $\Gamma H(\mathbf{k}) \Gamma^{-1} = -H(\mathbf{k})$ with $\Gamma = \sigma_z$ by construction. When the non-Hermitian Hamiltonian $H(\mathbf{k})$ has a point gap, the Hermitized Hamiltonian $\tilde{H}(\mathbf{k})$ is gapped, and vice versa. Thus, the topological classification of $H(\mathbf{k})$ coincides with that of $\tilde{H}(\mathbf{k})$, which is denoted by K_P . By contrast, the presence of a line gap imposes an additional constraint on $\tilde{H}(\mathbf{k})$. In fact, a non-Hermitian Hamiltonian $H(\mathbf{k})$ with a real or an imaginary line gap is continuously deformable to a

Hermitian or an anti-Hermitian Hamiltonian while keeping the line gap and relevant symmetry, respectively [36]. Notably, Hermiticity or anti-Hermiticity of $H(\mathbf{k})$ imposes another chiral symmetry with $\Gamma_r = \sigma_y$ or $\Gamma_i = \sigma_x$ on the Hermitized Hamiltonian $\tilde{H}(\mathbf{k})$, respectively. This additional chiral symmetry leads to the different topological classification K_{L_r} or K_{L_i} in the presence of a real or an imaginary line gap (and a point gap as well). Forgetting Γ_r (Γ_i) defines a homomorphism $f_r : K_{L_r} \rightarrow K_P$ ($f_i : K_{L_i} \rightarrow K_P$) from K_{L_r} (K_{L_i}) to K_P . Owing to the dimensional isomorphism of the K -theory, it is sufficient to compute f_r or f_i in zero dimension to obtain those in arbitrary dimensions. Table S1 summarizes these homomorphisms in the Altland-Zirnbauer[†] symmetry classes, which is relevant to this work. See Refs. [46, 85] for the homomorphisms in all the 38-fold symmetry classes.

If a point-gapped non-Hermitian Hamiltonian $H(\mathbf{k})$ is included in the image of either homomorphism f_r or f_i , it is continuously deformable to a Hermitian or an anti-Hermitian Hamiltonian, implying that the topological nature is also attributed to the conventional Hermitian one. Conversely, if $H(\mathbf{k})$ is not included in the image of f_r or f_i , its topological nature is intrinsic to non-Hermitian systems. Such intrinsic non-Hermitian topology is captured by the quotient group $K_P / (\text{Im } f_r \cup \text{Im } f_i)$, which is also summarized in Table S1. For example, point-gap topology in one-dimensional class A is intrinsic to non-Hermitian systems, while point-gap topology in two-dimensional class AIII is reducible to anti-Hermitian systems and hence of extrinsic nature.

TABLE S1. Homomorphisms f_r, f_i from line-gap to point-gap topology for the tenfold Altland-Zirnbauer[†] classification.

Class	Gap	$d = 0$	$d = 1$	$d = 2$	$d = 3$	$d = 4$	$d = 5$	$d = 6$	$d = 7$
A	$L \rightarrow P$	$\mathbb{Z} \rightarrow 0$	$0 \rightarrow \mathbb{Z}$	$\mathbb{Z} \rightarrow 0$	$0 \rightarrow \mathbb{Z}$	$\mathbb{Z} \rightarrow 0$	$0 \rightarrow \mathbb{Z}$	$\mathbb{Z} \rightarrow 0$	$0 \rightarrow \mathbb{Z}$
AIII	$L_r \rightarrow P$	$0 \rightarrow \mathbb{Z}$	$\mathbb{Z} \rightarrow 0$	$0 \rightarrow \mathbb{Z}$	$\mathbb{Z} \rightarrow 0$	$0 \rightarrow \mathbb{Z}$	$\mathbb{Z} \rightarrow 0$	$0 \rightarrow \mathbb{Z}$	$\mathbb{Z} \rightarrow 0$
	$L_i \rightarrow P$	$\mathbb{Z} \oplus \mathbb{Z} \rightarrow \mathbb{Z}$ $(n, m) \mapsto n - m$	$0 \rightarrow 0$	$\mathbb{Z} \oplus \mathbb{Z} \rightarrow \mathbb{Z}$ $(n, m) \mapsto n - m$	$0 \rightarrow 0$	$\mathbb{Z} \oplus \mathbb{Z} \rightarrow \mathbb{Z}$ $(n, m) \mapsto n - m$	$0 \rightarrow 0$	$\mathbb{Z} \oplus \mathbb{Z} \rightarrow \mathbb{Z}$ $(n, m) \mapsto n - m$	$0 \rightarrow 0$
AI [†]	$L \rightarrow P$	$\mathbb{Z} \rightarrow 0$	$0 \rightarrow 0$	$0 \rightarrow 0$	$0 \rightarrow 2\mathbb{Z}$	$2\mathbb{Z} \rightarrow 0$	$0 \rightarrow \mathbb{Z}_2$	$\mathbb{Z}_2 \rightarrow \mathbb{Z}_2$ $n \mapsto 0$	$\mathbb{Z}_2 \rightarrow \mathbb{Z}$
BDI [†]	$L_r \rightarrow P$	$\mathbb{Z}_2 \rightarrow \mathbb{Z}$	$\mathbb{Z} \rightarrow 0$	$0 \rightarrow 0$	$0 \rightarrow 0$	$0 \rightarrow 2\mathbb{Z}$	$2\mathbb{Z} \rightarrow 0$	$0 \rightarrow \mathbb{Z}_2$	$\mathbb{Z}_2 \rightarrow \mathbb{Z}_2$ $n \mapsto 0$
	$L_i \rightarrow P$	$\mathbb{Z} \oplus \mathbb{Z} \rightarrow \mathbb{Z}$ $(n, m) \mapsto n - m$	$0 \rightarrow 0$	$0 \rightarrow 0$	$0 \rightarrow 0$	$2\mathbb{Z} \oplus 2\mathbb{Z} \rightarrow 2\mathbb{Z}$ $(n, m) \mapsto n - m$	$0 \rightarrow 0$	$\mathbb{Z}_2 \oplus \mathbb{Z}_2 \rightarrow \mathbb{Z}_2$ $(n, m) \mapsto n + m$	$\mathbb{Z}_2 \oplus \mathbb{Z}_2 \rightarrow \mathbb{Z}_2$ $(n, m) \mapsto n + m$
D [†]	$L_r \rightarrow P$	$\mathbb{Z}_2 \rightarrow \mathbb{Z}_2$ $n \mapsto 0$	$\mathbb{Z}_2 \rightarrow \mathbb{Z}$	$\mathbb{Z} \rightarrow 0$	$0 \rightarrow 0$	$0 \rightarrow 0$	$0 \rightarrow 2\mathbb{Z}$	$2\mathbb{Z} \rightarrow 0$	$0 \rightarrow \mathbb{Z}_2$
	$L_i \rightarrow P$	$\mathbb{Z} \rightarrow \mathbb{Z}_2$ $n \mapsto n$	$0 \rightarrow \mathbb{Z}$	$0 \rightarrow 0$	$0 \rightarrow 0$	$2\mathbb{Z} \rightarrow 0$	$0 \rightarrow 2\mathbb{Z}$	$\mathbb{Z}_2 \rightarrow 0$	$\mathbb{Z}_2 \rightarrow \mathbb{Z}_2$ $n \mapsto n$
DIII [†]	$L_r \rightarrow P$	$0 \rightarrow \mathbb{Z}_2$	$\mathbb{Z}_2 \rightarrow \mathbb{Z}_2$ $n \mapsto 0$	$\mathbb{Z}_2 \rightarrow \mathbb{Z}$	$\mathbb{Z} \rightarrow 0$	$0 \rightarrow 0$	$0 \rightarrow 0$	$0 \rightarrow 2\mathbb{Z}$	$2\mathbb{Z} \rightarrow 0$
	$L_i \rightarrow P$	$\mathbb{Z} \rightarrow \mathbb{Z}_2$ $n \mapsto n$	$0 \rightarrow \mathbb{Z}_2$	$\mathbb{Z} \rightarrow \mathbb{Z}$ $n \mapsto 2n$	$0 \rightarrow 0$	$\mathbb{Z} \rightarrow 0$	$0 \rightarrow 0$	$\mathbb{Z} \rightarrow 2\mathbb{Z}$ $n \mapsto n$	$0 \rightarrow 0$
AII [†]	$L \rightarrow P$	$2\mathbb{Z} \rightarrow 0$	$0 \rightarrow \mathbb{Z}_2$	$\mathbb{Z}_2 \rightarrow \mathbb{Z}_2$ $n \mapsto 0$	$\mathbb{Z}_2 \rightarrow \mathbb{Z}$	$\mathbb{Z} \rightarrow 0$	$0 \rightarrow 0$	$0 \rightarrow 0$	$0 \rightarrow 2\mathbb{Z}$
CII [†]	$L_r \rightarrow P$	$0 \rightarrow 2\mathbb{Z}$	$2\mathbb{Z} \rightarrow 0$	$0 \rightarrow \mathbb{Z}_2$	$\mathbb{Z}_2 \rightarrow \mathbb{Z}_2$ $n \mapsto 0$	$\mathbb{Z}_2 \rightarrow \mathbb{Z}$	$\mathbb{Z} \rightarrow 0$	$0 \rightarrow 0$	$0 \rightarrow 0$
	$L_i \rightarrow P$	$2\mathbb{Z} \oplus 2\mathbb{Z} \rightarrow 2\mathbb{Z}$ $(n, m) \mapsto n - m$	$0 \rightarrow 0$	$\mathbb{Z}_2 \oplus \mathbb{Z}_2 \rightarrow \mathbb{Z}_2$ $(n, m) \mapsto n + m$	$\mathbb{Z}_2 \oplus \mathbb{Z}_2 \rightarrow \mathbb{Z}_2$ $(n, m) \mapsto n + m$	$\mathbb{Z} \oplus \mathbb{Z} \rightarrow \mathbb{Z}$ $(n, m) \mapsto n - m$	$0 \rightarrow 0$	$0 \rightarrow 0$	$0 \rightarrow 0$
C [†]	$L_r \rightarrow P$	$0 \rightarrow 0$	$0 \rightarrow 2\mathbb{Z}$	$2\mathbb{Z} \rightarrow 0$	$0 \rightarrow \mathbb{Z}_2$	$\mathbb{Z}_2 \rightarrow \mathbb{Z}_2$ $n \mapsto 0$	$\mathbb{Z}_2 \rightarrow \mathbb{Z}$	$\mathbb{Z} \rightarrow 0$	$0 \rightarrow 0$
	$L_i \rightarrow P$	$2\mathbb{Z} \rightarrow 0$	$0 \rightarrow 2\mathbb{Z}$	$\mathbb{Z}_2 \rightarrow 0$	$\mathbb{Z}_2 \rightarrow \mathbb{Z}_2$ $n \mapsto n$	$\mathbb{Z} \rightarrow \mathbb{Z}_2$ $n \mapsto n$	$0 \rightarrow \mathbb{Z}$	$0 \rightarrow 0$	$0 \rightarrow 0$
CI [†]	$L_r \rightarrow P$	$0 \rightarrow 0$	$0 \rightarrow 0$	$0 \rightarrow 2\mathbb{Z}$	$2\mathbb{Z} \rightarrow 0$	$0 \rightarrow \mathbb{Z}_2$	$\mathbb{Z}_2 \rightarrow \mathbb{Z}_2$ $n \mapsto 0$	$\mathbb{Z}_2 \rightarrow \mathbb{Z}$	$\mathbb{Z} \rightarrow 0$
	$L_i \rightarrow P$	$\mathbb{Z} \rightarrow 0$	$0 \rightarrow 0$	$\mathbb{Z} \rightarrow 2\mathbb{Z}$ $n \mapsto n$	$0 \rightarrow 0$	$\mathbb{Z} \rightarrow \mathbb{Z}_2$ $n \mapsto n$	$0 \rightarrow \mathbb{Z}_2$	$\mathbb{Z} \rightarrow \mathbb{Z}$ $n \mapsto 2n$	$0 \rightarrow 0$

VI. FROM ALTLAND-ZIRNBAUER CLASSIFICATION TO WIGNER-DYSON CLASSIFICATION

We provide homomorphisms from topological phases in the tenfold Altland-Zirnbauer (AZ) symmetry classes to those in the threefold Wigner-Dyson (WD) classes (A, AI, and AII). Let us first introduce the topological invariants for the AZ classification. As summarized in Table S2, each nontrivial d -dimensional topological phase is characterized by one of $\{W_d, \text{Ch}_{d/2}, \text{FK}_{d/2}, \text{CS}_d, \widetilde{\text{CS}}_d\}$, which are the d -dimensional winding number, the $d/2$ -th Chern number, the Fu-Kane invariant, and the Chern-Simons invariant in symmetry classes without (with) chiral symmetry, respectively [6]. The homomorphisms are given in Table S3, based on the connections among these topological invariants, i.e., how the d -dimensional topological invariants in the AZ classes relate to those in the WD classes if one virtually forgets particle-hole symmetry and/or chiral symmetry. To derive these homomorphisms, we divide all the entries in Table S3 into the following seven categories. We identify

the homomorphism for each case below.

1. $\{\mathbb{Z}^\vee \xrightarrow{\cong} \mathbb{Z}, \mathbb{Z}^\vee \xrightarrow{\cong} 2\mathbb{Z}, \mathbb{Z}_2^\vee \xrightarrow{\cong} \mathbb{Z}_2\}$

Let us focus on class DIII in two dimensions to explain how to see and prove Table S3. Since class DIII respects spin-full time-reversal symmetry, it reduces to class AII if one ignores both particle-hole and chiral symmetry. See the first four columns of Table S2 and Table S3. The entries $\mathbb{Z}_2^\vee \xrightarrow{\cong} \mathbb{Z}_2$ show how the topological phase in class DIII, the left side of the arrow (i.e., \mathbb{Z}_2^\vee), is mapped to that in class AII, the right side of the arrow (i.e., \mathbb{Z}_2). Since, for two dimensions, both the \mathbb{Z}_2 invariants coincide and are given by the Fu-Kane invariant FK_1 (see Table S2) [90], we conclude that the nontrivial topological phase in 2D class DIII is isomorphically mapped to that in two-dimensional class AII. We use the symbol “ \cong ” in $\mathbb{Z}_2^\vee \xrightarrow{\cong} \mathbb{Z}_2$ to emphasize that this homomorphism is indeed an (group) isomorphism. In a similar manner to this, we have an isomorphism for each of $\{\mathbb{Z}^\vee \xrightarrow{\cong} \mathbb{Z}, \mathbb{Z}^\vee \xrightarrow{\cong} 2\mathbb{Z}, \mathbb{Z}_2^\vee \xrightarrow{\cong} \mathbb{Z}_2\}$ in Table S3.

2. $\{\mathbb{Z}^\vee \xrightarrow{2} \mathbb{Z}\}$

The entries $\mathbb{Z}^\vee \xrightarrow{2} \mathbb{Z}$ appear in two-dimensional class C and six-dimensional class D. These two classes reduce to class A when one forgets particle-hole symmetry. In two dimensions, the first Chern number characterizes both classes A and C, where the presence of particle-hole symmetry makes it even integers. Thus, we have a map from the topological phases in two-dimensional class C to the even parts of those in two-dimensional class A. We denote this homomorphism by $\mathbb{Z}^\vee \xrightarrow{2} \mathbb{Z}$. Similarly, one can show this kind of map for six-dimensional class D.

3. $\{\mathbb{Z}^\vee / \times \xrightarrow{\text{mod } 2} \mathbb{Z}_2\}$

In three dimensions, we have the entry $\mathbb{Z}^\vee / \times \xrightarrow{\text{mod } 2} \mathbb{Z}_2$ for class DIII. Since the corresponding WD symmetry class is class AII, what we should know is the connection between the three-dimensional winding number W_3 and the Chern-Simons invariant CS_3 (see Table S2). Notably, W_d relates to CS_d through $(-1)^{W_d} = (-1)^{\text{CS}_d}$ for general odd d spatial dimensions [6]. Therefore, only the even parts of topological phases in three-dimensional class DIII are sent to the nontrivial phase in three-dimensional class AII. This homomorphism is written as $\mathbb{Z}^\vee / \times \xrightarrow{\text{mod } 2} \mathbb{Z}_2$. One can also prove the presence of such a “mod 2” map for seven-dimensional class CI in the same manner.

4. $\{\mathbb{Z}_2^\times \xrightarrow{0} \mathbb{Z}\}$

Because we consider homomorphisms that preserve the group structure, only the possible map from the \mathbb{Z}_2 classification to the \mathbb{Z} classification is a zero map. In fact, all elements of the \mathbb{Z}_2 topological phases are sent to a trivial one in the \mathbb{Z} topological phases. We use the symbol $\mathbb{Z}_2^\times \xrightarrow{0} \mathbb{Z}$ to represent this zero-map homomorphism. For instance, in four dimensions, the Fu-Kane invariant FK_2 for class CII does not result in the nontrivial values of the second Chern number Ch_2 for class AII if one ignores both particle-hole symmetry and chiral symmetry.

5. $\{\mathbb{Z}_2^\times \xrightarrow{0} \mathbb{Z}_2\}$

The entries $\mathbb{Z}_2^\times \xrightarrow{0} \mathbb{Z}_2$ show that all the topological phases in the original AZ classes are mapped to a trivial phase in the corresponding WD classes. We show this using the dimensional reduction of topological phases [91]. Let us consider three-dimensional class CII as an example. This class is characterized by the Chern-Simons invariant $\widetilde{\text{CS}}_3$, while the corresponding WD class (i.e., class AII) is characterized by the other type of Chern-Simons invariant CS_3 . The dimensional reduction connects the \mathbb{Z}_2 descendants to their parent \mathbb{Z} topology in each complex symmetry class. For the present case, $(-1)^{\widetilde{\text{CS}}_3} = (-1)^{\text{FK}_2} = (-1)^{W_5}$ holds for class CII in $d = 3, 4, 5$. Similarly, we have $(-1)^{\text{FK}_1} = (-1)^{\text{CS}_3} = (-1)^{\text{Ch}_2}$ for class AII in $d = 2, 3, 4$. See Table S2. As stated in the previous case, FK_2 in four-dimensional class CII always leads to a trivial value of Ch_2 in four-dimensional class AII. Combining this with the dimensional reduction in $d = 3, 4$, we conclude that $\widetilde{\text{CS}}_3$ only relates to trivial CS_3 . Similarly, one can prove this kind of zero map for other classes.

6. $\{\mathbb{Z}^\times \rightarrow 0, \mathbb{Z}^\times \rightarrow 0, \mathbb{Z}_2^\times \rightarrow 0\}$

Since the corresponding WD classes have no nontrivial topological phases, the homomorphisms are just zero maps. Here, we do not use the symbol “ $\xrightarrow{0}$ ” like the previous two cases as the homomorphisms are clearly zero maps.

7. $\{0 \rightarrow 0, 0 \rightarrow \mathbb{Z}, 0 \rightarrow 2\mathbb{Z}, 0 \rightarrow \mathbb{Z}_2\}$

Since the original AZ classes are topologically trivial, the homomorphisms are given by zero maps to retain the group structure. Here, we do not use the symbol “ $\xrightarrow{0}$ ” to express the zero maps.

TABLE S2. Topological invariants for the tenfold Altland-Zirnbauer classes. There exist four types of invariants: For the \mathbb{Z} indices, “ W_d ” is the d -dimensional winding number and “ $\text{Ch}_{d/2}$ ” is the $d/2$ -th Chern number, which are defined in odd and even d spatial dimensions, respectively. For the \mathbb{Z}_2 indices, “ $\text{FK}_{d/2}$ ” denotes the Fu-Kane invariant in even d dimensions, and “ CS_d ($\widetilde{\text{CS}}_d$)” represents the Chern-Simons invariant in symmetry classes without (with) chiral symmetry in odd d dimensions. Note that the entries “0” indicate the absence of nontrivial topological phases.

Class	TRS	PHS	CS	$d = 1$	$d = 2$	$d = 3$	$d = 4$	$d = 5$	$d = 6$	$d = 7$	$d = 8$
A	0	0	0	0	$\text{Ch}_1 \in \mathbb{Z}^\vee$	0	$\text{Ch}_2 \in \mathbb{Z}^\vee$	0	$\text{Ch}_3 \in \mathbb{Z}^\vee$	0	$\text{Ch}_4 \in \mathbb{Z}^\vee$
AIII	0	0	1	$W_1 \in \mathbb{Z}^\times$	0	$W_3 \in \mathbb{Z}^\times$	0	$W_5 \in \mathbb{Z}^\times$	0	$W_7 \in \mathbb{Z}^\times$	0
AI	+1	0	0	0	0	0	$\text{Ch}_2 \in 2\mathbb{Z}^\vee$	0	$\text{FK}_3 \in \mathbb{Z}_2^\vee$	$\text{CS}_7 \in \mathbb{Z}_2^\vee$	$\text{Ch}_4 \in \mathbb{Z}^\vee$
BDI	+1	+1	1	$W_1 \in \mathbb{Z}^\times$	0	0	0	$W_5 \in 2\mathbb{Z}^\times$	0	$\widetilde{\text{CS}}_7 \in \mathbb{Z}_2^\times$	$\text{FK}_4 \in \mathbb{Z}_2^\times$
D	0	+1	0	$\text{CS}_1 \in \mathbb{Z}_2^\times$	$\text{Ch}_1 \in \mathbb{Z}^\vee$	0	0	0	$\text{Ch}_3 \in 2\mathbb{Z}^\vee$	0	$\text{FK}_4 \in \mathbb{Z}_2^\times$
DIII	-1	+1	1	$\widetilde{\text{CS}}_1 \in \mathbb{Z}_2^\times$	$\text{FK}_1 \in \mathbb{Z}_2^\vee$	$W_3 \in \mathbb{Z}^\vee/\times$	0	0	0	$W_7 \in 2\mathbb{Z}^\times$	0
AII	-1	0	0	0	$\text{FK}_1 \in \mathbb{Z}_2^\vee$	$\text{CS}_3 \in \mathbb{Z}_2^\vee$	$\text{Ch}_2 \in \mathbb{Z}^\vee$	0	0	0	$\text{Ch}_4 \in 2\mathbb{Z}^\vee$
CII	-1	-1	1	$W_1 \in 2\mathbb{Z}^\times$	0	$\widetilde{\text{CS}}_3 \in \mathbb{Z}_2^\times$	$\text{FK}_2 \in \mathbb{Z}_2^\times$	$W_5 \in \mathbb{Z}^\times$	0	0	0
C	0	-1	0	0	$\text{Ch}_1 \in 2\mathbb{Z}^\vee$	0	$\text{FK}_2 \in \mathbb{Z}_2^\times$	$\text{CS}_5 \in \mathbb{Z}_2^\times$	$\text{Ch}_3 \in \mathbb{Z}^\vee$	0	0
CI	+1	-1	1	0	0	$W_3 \in 2\mathbb{Z}^\times$	0	$\widetilde{\text{CS}}_5 \in \mathbb{Z}_2^\times$	$\text{FK}_3 \in \mathbb{Z}_2^\vee$	$W_7 \in \mathbb{Z}^\vee/\times$	0

TABLE S3. Homomorphisms from the tenfold Altland-Zirnbauer (AZ) symmetry classification to the threefold Wigner-Dyson (WD) classification. While the tenfold AZ classes are specified by time-reversal symmetry (TRS), particle-hole symmetry (PHS), and chiral symmetry (CS), the threefold WD classes are based solely on TRS. For the entries “ $\mathbb{Z}^\vee \xrightarrow{\cong} \mathbb{Z}$ ”, “ $2\mathbb{Z}^\vee \xrightarrow{\cong} 2\mathbb{Z}$ ”, and “ $\mathbb{Z}_2^\vee \xrightarrow{\cong} \mathbb{Z}_2$ ”, the original topological phases in the AZ classes are isomorphic to those in the corresponding WD classes. For the entries “ $\mathbb{Z}_2^\times \xrightarrow{0} \mathbb{Z}_2$ ” and “ $\mathbb{Z}_2^\times \xrightarrow{0} \mathbb{Z}$ ”, the original topological phases in the AZ classes vanish in the corresponding WD classes. For the entries “ $2\mathbb{Z}^\vee \xrightarrow{2} \mathbb{Z}$ ”, the topological invariants double. For the entries “ $\mathbb{Z}^\vee/\times \xrightarrow{\text{mod } 2} \mathbb{Z}_2$ ”, the topological phases with the odd (even) number of topological invariants survive (vanish).

Class	TRS	PHS	CS	$d = 1$	$d = 2$	$d = 3$	$d = 4$	$d = 5$	$d = 6$	$d = 7$	$d = 8$
A \rightarrow A	0	0	0	$0 \rightarrow 0$	$\mathbb{Z}^\vee \xrightarrow{\cong} \mathbb{Z}$	$0 \rightarrow 0$	$\mathbb{Z}^\vee \xrightarrow{\cong} \mathbb{Z}$	$0 \rightarrow 0$	$\mathbb{Z}^\vee \xrightarrow{\cong} \mathbb{Z}$	$0 \rightarrow 0$	$\mathbb{Z}^\vee \xrightarrow{\cong} \mathbb{Z}$
AIII \rightarrow A	0	0	1	$\mathbb{Z}^\times \rightarrow 0$	$0 \rightarrow \mathbb{Z}$	$\mathbb{Z}^\times \rightarrow 0$	$0 \rightarrow \mathbb{Z}$	$\mathbb{Z}^\times \rightarrow 0$	$0 \rightarrow \mathbb{Z}$	$\mathbb{Z}^\times \rightarrow 0$	$0 \rightarrow \mathbb{Z}$
AI \rightarrow AI	+1	0	0	$0 \rightarrow 0$	$0 \rightarrow 0$	$0 \rightarrow 0$	$2\mathbb{Z}^\vee \xrightarrow{\cong} 2\mathbb{Z}$	$0 \rightarrow 0$	$\mathbb{Z}_2^\vee \xrightarrow{\cong} \mathbb{Z}_2$	$\mathbb{Z}_2^\vee \xrightarrow{\cong} \mathbb{Z}_2$	$\mathbb{Z}^\vee \xrightarrow{\cong} \mathbb{Z}$
BDI \rightarrow AI	+1	+1	1	$\mathbb{Z}^\times \rightarrow 0$	$0 \rightarrow 0$	$0 \rightarrow 0$	$0 \rightarrow 2\mathbb{Z}$	$2\mathbb{Z}^\times \rightarrow 0$	$0 \rightarrow \mathbb{Z}_2$	$\mathbb{Z}_2^\times \xrightarrow{0} \mathbb{Z}_2$	$\mathbb{Z}_2^\times \xrightarrow{0} \mathbb{Z}$
D \rightarrow A	0	+1	0	$\mathbb{Z}_2^\times \rightarrow 0$	$\mathbb{Z}^\vee \xrightarrow{\cong} \mathbb{Z}$	$0 \rightarrow 0$	$0 \rightarrow \mathbb{Z}$	$0 \rightarrow 0$	$2\mathbb{Z}^\vee \xrightarrow{2} \mathbb{Z}$	$0 \rightarrow 0$	$\mathbb{Z}_2^\times \xrightarrow{0} \mathbb{Z}$
DIII \rightarrow AII	-1	+1	1	$\mathbb{Z}_2^\times \rightarrow 0$	$\mathbb{Z}_2^\vee \xrightarrow{\cong} \mathbb{Z}_2$	$\mathbb{Z}^\vee/\times \xrightarrow{\text{mod } 2} \mathbb{Z}_2$	$0 \rightarrow \mathbb{Z}$	$0 \rightarrow 0$	$0 \rightarrow 0$	$2\mathbb{Z}^\times \rightarrow 0$	$0 \rightarrow 2\mathbb{Z}$
AII \rightarrow AII	-1	0	0	$0 \rightarrow 0$	$\mathbb{Z}_2^\vee \xrightarrow{\cong} \mathbb{Z}_2$	$\mathbb{Z}_2^\vee \xrightarrow{\cong} \mathbb{Z}_2$	$\mathbb{Z}^\vee \xrightarrow{\cong} \mathbb{Z}$	$0 \rightarrow 0$	$0 \rightarrow 0$	$0 \rightarrow 0$	$2\mathbb{Z}^\vee \xrightarrow{\cong} 2\mathbb{Z}$
CII \rightarrow AII	-1	-1	1	$2\mathbb{Z}^\times \rightarrow 0$	$0 \rightarrow \mathbb{Z}_2$	$\mathbb{Z}_2^\times \xrightarrow{0} \mathbb{Z}_2$	$\mathbb{Z}_2^\times \xrightarrow{0} \mathbb{Z}$	$\mathbb{Z}^\times \rightarrow 0$	$0 \rightarrow 0$	$0 \rightarrow 0$	$0 \rightarrow 2\mathbb{Z}$
C \rightarrow A	0	-1	0	$0 \rightarrow 0$	$2\mathbb{Z}^\vee \xrightarrow{2} \mathbb{Z}$	$0 \rightarrow 0$	$\mathbb{Z}_2^\times \xrightarrow{0} \mathbb{Z}$	$\mathbb{Z}_2^\times \rightarrow 0$	$\mathbb{Z}^\vee \xrightarrow{\cong} \mathbb{Z}$	$0 \rightarrow 0$	$0 \rightarrow \mathbb{Z}$
CI \rightarrow AI	+1	-1	1	$0 \rightarrow 0$	$0 \rightarrow 0$	$2\mathbb{Z}^\times \rightarrow 0$	$0 \rightarrow 2\mathbb{Z}$	$\mathbb{Z}_2^\times \rightarrow 0$	$\mathbb{Z}_2^\vee \xrightarrow{\cong} \mathbb{Z}_2$	$\mathbb{Z}^\vee/\times \xrightarrow{\text{mod } 2} \mathbb{Z}_2$	$0 \rightarrow \mathbb{Z}$

VII. K-THEORY PERSPECTIVE

We classified the detached boundary states as extrinsic non-Hermitian topology in Sec. V and Wannier localizability in Sec. VI. These two results give the same classification. In this section, we discuss why the two approaches coincide from the viewpoint of K -theory. The discussion in this section applies to any magnetic space group symmetry compatible with planar boundary conditions.

The degree +1 K -group K^1 is represented by self-adjoint Fredholm operators whose essential spectrum contains both positive and negative values [94]. Gapless Hamiltonians naturally represent such operators realized in topological surface states, meaning that there exists an energy gap $E_{\text{gap}} > 0$ with a finite number of surface-state spectra in $E \in [-E_{\text{gap}}, E_{\text{gap}}]$ and an infinite number of bulk spectra outside this range.

Let $\hat{H}(\mathbf{k}_{\parallel})$ be the infinite-dimensional gapless Hamiltonian on the surface Brillouin zone T^{d-1} , where $\mathbf{k}_{\parallel} \in T^{d-1}$, \mathcal{G} be the symmetry group compatible with the presence of the surface, $\Pi \cong \mathbb{Z}^{d-1}$ be the lattice translation subgroup, and $G = \mathcal{G}/\Pi$ be their quotient group. The group G acts on the surface Brillouin zone as $g : \mathbf{k}_{\parallel} \mapsto g\mathbf{k}_{\parallel}$. We use the homomorphism $\phi, c : G \rightarrow \{\pm 1\}$ to specify unitary ($\phi_g = 1$) or antiunitary ($\phi_g = -1$) symmetries, and conventional ($c_g = 1$) or anti- ($c_g = -1$) symmetries (Antisymmetry changes the sign of Hamiltonian. Chiral symmetry and particle-hole symmetry are prime examples of antisymmetry.) For matrices M , we also introduce the notation M^{ϕ_g} as M when $\phi_g = 1$ and M^* when $\phi_g = -1$.

Then, we can summarize symmetry algebra among symmetry operators in G as

$$u_g(h\mathbf{k}_{\parallel})u_h(\mathbf{k}_{\parallel})^{\phi_g} = \tau_{g,h}(gh\mathbf{k}_{\parallel})u_{gh}(\mathbf{k}_{\parallel}), \quad g, h \in G, \quad (\text{VII.1})$$

where $u_g(\mathbf{k}_{\parallel})$ is a unitary operator for $g \in G$. Here, τ is a 2-cocycle $\tau \in Z_{\text{group}}^2(G, C(T^{d-1}, U(1)))$, where $C(T^{d-1}, U(1))$ is the group of $U(1)$ -valued functions on T^{d-1} with a left G -action defined by $(g.\tau)(\mathbf{k}_{\parallel}) = \tau(g^{-1}\mathbf{k}_{\parallel})$. The twisted equivariant K -group ${}^{\phi}K_G^{(\tau,c)+1}(T^{d-1})$ [95, 98] classify the topology of $(d-1)$ gapless Hamiltonians with the following symmetries:

$$u_g(\mathbf{k}_{\parallel})\hat{H}(\mathbf{k}_{\parallel})^{\phi_g}u_g(\mathbf{k}_{\parallel})^{\dagger} = c_g\hat{H}(g\mathbf{k}_{\parallel}), \quad g \in G. \quad (\text{VII.2})$$

First, we relate the gapless Hamiltonian to a point-gapped Hamiltonian: $\chi(E)$ be a continuous odd function satisfying $\chi(E) = \text{sgn}(E)$ for $|E| > E_{\text{gap}}$ and $\chi(E) = E/E_{\text{gap}}$ for $|E| \leq E_{\text{gap}}$. From the gapless Hamiltonian $\hat{H}(\mathbf{k}_{\parallel})$, we obtain the point-gapped Hamiltonian $H_P(\mathbf{k}_{\parallel})$ by

$$H_P(\mathbf{k}_{\parallel}) := i \exp\left(-i\pi\chi\left(\hat{H}(\mathbf{k}_{\parallel})\right)\right). \quad (\text{VII.3})$$

It is found that the point-gapped Hamiltonian $H_{\mathbf{k}}$ satisfies the following symmetries,

$$u_g(\mathbf{k}_{\parallel})H_P(\mathbf{k}_{\parallel})^{\phi_g}u_g(\mathbf{k}_{\parallel})^{\dagger} = c_g \begin{cases} H_P(g\mathbf{k}_{\parallel}) & (\phi_g c_g = 1); \\ H_P(g\mathbf{k}_{\parallel})^{\dagger} & (\phi_g c_g = -1). \end{cases} \quad (\text{VII.4})$$

In other words, the point-gapped Hamiltonian shares the same unitary symmetries with the original gapless Hamiltonian, but it realizes other symmetries in a different manner. In particular, it hosts Altland-Zirnbauer^{dagger} symmetries, instead of the original Altland-Zirnbauer symmetries. Importantly, this map ensures that the K -group ${}^{\phi}K_G^{(\tau,c)+1}(T^{d-1})$ also classify the topology of point-gapped Hamiltonians satisfying symmetry in Eq. (VII.4).

We also use another equivalent relation between Hermitian and non-Hermitian topologies. For the point-gapped Hamiltonian in Eq.(VII.3),

$$\tilde{H}(\mathbf{k}_{\parallel}) = \begin{pmatrix} 0 & H_P(\mathbf{k}_{\parallel}) \\ H_P(\mathbf{k}_{\parallel})^{\dagger} & 0 \end{pmatrix}_{\sigma}, \quad (\text{VII.5})$$

which is gapped because $\tilde{H}(\mathbf{k}_{\parallel})^2 = 1$. By design, $\tilde{H}(\mathbf{k}_{\parallel})$ has chiral symmetry

$$\sigma_z \tilde{H}(\mathbf{k}_{\parallel}) = -\tilde{H}(\mathbf{k}_{\parallel}) \sigma_z. \quad (\text{VII.6})$$

The symmetry constraints in Eq. (VII.4) are mapped as

$$\tilde{u}_g(\mathbf{k}_{\parallel})\tilde{H}(\mathbf{k}_{\parallel})^{\phi_g}\tilde{u}_g(\mathbf{k}_{\parallel})^{\dagger} = c_g\tilde{H}(g\mathbf{k}_{\parallel}), \quad \tilde{u}_g(\mathbf{k}_{\parallel}) = u_g(\mathbf{k}_{\parallel}) \otimes (\sigma_x)^{\frac{1-\phi_g c_g}{2}}, \quad g \in G. \quad (\text{VII.7})$$

They satisfy the following algebraic relation with chiral symmetry:

$$(i\sigma_z)^2 = -1, \quad \tilde{u}_g(\mathbf{k}_{\parallel})(i\sigma_z)^{\phi_g} = c_g(i\sigma_z)\tilde{u}_g(\mathbf{k}_{\parallel}), \quad g \in G. \quad (\text{VII.8})$$

If chiral symmetry in Eq.(VII.6) is absent, then the gapped Hamiltonian with G symmetry in Eq. (VII.7) gives the degree 0 K -group ${}^{\phi}K_G^{(\tau,c)+0}(T^{d-1})$. Additional chiral symmetry satisfying the algebraic relation in Eq. (VII.8) increases the degree of the K -group by +1 [93] and thus, the Hermitian Hamiltonian $\tilde{H}(\mathbf{k}_{\parallel})$ gives the same K -group ${}^{\phi}K_G^{(\tau,c)+1}(T^{d-1})$ as the point-gapped Hamiltonian.

For a point-gapped Hamiltonian $H_P(\mathbf{k}_{\parallel})$, imposing the imaginary line gap (i.e., the spectrum of $H_P(\mathbf{k}_{\parallel})$ does not contain $\text{Re } E = 0$) is equivalent to imposing the anti-Hermitian condition $H_P(\mathbf{k}_{\parallel})^{\dagger} = -H_P(\mathbf{k}_{\parallel})$ on $H_P(\mathbf{k}_{\parallel})$ [46]. Moreover, this is also equivalent to imposing chiral symmetry σ_x on the gapped Hermitianized Hamiltonian $\tilde{H}(\mathbf{k}_{\parallel})$ in addition to Eqs. (VII.6) and (VII.7):

$$\sigma_x \tilde{H}(\mathbf{k}_{\parallel}) = -\tilde{H}(\mathbf{k}_{\parallel}) \sigma_x. \quad (\text{VII.9})$$

Using the chiral operator σ_x , we construct a Hamiltonian parameterized by the interval $I = [-1, 1]$ as

$$\tilde{H}'(\mathbf{k}_{\parallel}, t) = \sin \frac{\pi t}{2} \sigma_x + \cos \frac{\pi t}{2} \tilde{H}(\mathbf{k}_{\parallel}), \quad t \in I. \quad (\text{VII.10})$$

It should be noted that the symmetry group G acts on the additional parameter space as $c_g t$,

$$\tilde{u}_g(\mathbf{k}_{\parallel}) \tilde{H}'(\mathbf{k}_{\parallel}, t) \tilde{u}_g(\mathbf{k}_{\parallel})^\dagger = c_g \tilde{H}'(g\mathbf{k}_{\parallel}, c_g t), \quad g \in G. \quad (\text{VII.11})$$

Therefore, the Hamiltonian $\tilde{H}'(\mathbf{k}_{\parallel}, t)$, and thus the imaginary-line-gapped phase, is classified by the relative K -group $\phi K_G^{(\tau, c)+1}(T^{d-1} \times I, T^{d-1} \times \partial I)$, where G acts on $T^{d-1} \times I$ as $g : (\mathbf{k}_{\parallel}, t) \mapsto (g\mathbf{k}_{\parallel}, c_g t)$, and $\partial I = \{-1, 1\}$ is the boundary of the interval. From the long exact sequence for the pair $(T^{d-1} \times I, T^{d-1} \times \partial I)$, we obtain the exact sequence

$$\phi K_G^{(\tau, c)+1}(T^{d-1} \times I, T^{d-1} \times \partial I) \xrightarrow{f_{L_i}^{\text{bdy}}} \phi K_G^{(\tau, c)+1}(T^{d-1}) \xrightarrow{f_0^{\text{bdy}}} \phi K_G^{(\tau, c)+1}(T^{d-1} \times \partial I). \quad (\text{VII.12})$$

We used the isomorphism $\phi K_G^{(\tau, c)+1}(T^{d-1} \times I) \cong \phi K_G^{(\tau, c)+1}(T^{d-1})$ due to the contractibility of the interval I . The exactness implies $\text{im } f_{L_i}^{\text{bdy}} = \ker f_0^{\text{bdy}}$. The homomorphism $f_{L_i}^{\text{bdy}}$ is the same map from imaginary-line-gapped phases to point-gapped phases introduced in Ref. [46]. If there are no group elements $g \in G$ with $c_g = -1$, the K -group $\phi K_G^{(\tau, c)+1}(T^{d-1} \times \partial I)$ reduces to two copies defined on two independent points $\{-1, 1\} = \partial I$, leading to:

$$\phi K_G^{\tau+1}(T^{d-1} \times I, T^{d-1} \times \partial I) \xrightarrow{f_{L_i}^{\text{bdy}}} \phi K_G^{\tau+1}(T^{d-1}) \xrightarrow{f_0^{\text{bdy}}} \phi K_G^{\tau+1}(T^{d-1})^{\oplus 2}. \quad (\text{VII.13})$$

Here, we dropped c since $c_g \equiv 1$ from the assumption. In this case, since f_0^{bdy} sends x to (x, x) , we have $\ker f_0^{\text{bdy}} = 0$, so $\text{im } f_{L_i}^{\text{bdy}} = 0$, meaning that there are no point-gapped phases representable by an imaginary-line-gapped phases. On the other hand, if there is a group element $g \in G$ with $c_g = -1$, g exchanges $t = 1$ and $t = -1$, so it merely relates the K -group at $t = 1$ with that at $t = -1$. Thus, we only need to consider the K -group at $t = 1$, excluding group elements with $c_g = 1$. This consideration gives the isomorphism $\phi K_G^{(\tau, c)+1}(T^{d-1} \times \partial I) \cong \phi K_{G_0}^{\tau+1}(T^{d-1})$, where $G_0 := \ker c = \{g \in G \mid c_g = 1\}$ is the subgroup of G excluding antisymmetries. As a result, we get

$$\phi K_G^{(\tau, c)+1}(T^{d-1} \times I, T^{d-1} \times \partial I) \xrightarrow{f_{L_i}^{\text{bdy}}} \phi K_G^{(\tau, c)+1}(T^{d-1}) \xrightarrow{f_0^{\text{bdy}}} \phi K_{G_0}^{\tau+1}(T^{d-1}). \quad (\text{VII.14})$$

Here, f_0^{bdy} in (VII.14) can be redefined as forgetting antisymmetries.

To derive Eqs.(VII.13) and (VII.14), we have assumed that the point gapped Hamiltonian $H_P(k_{\parallel})$ can be anti-Hermitian. Under the same assumption, we can obtain another useful expression for the K -group. For the anti-Hermitian point-gapped Hamiltonian $H_P(\mathbf{k}_{\parallel})$ (i.e., $H_P(\mathbf{k}_{\parallel})^\dagger = -H_P(\mathbf{k}_{\parallel})$), the symmetry constraints in Eq. (VII.4) are rewritten as

$$u_g(\mathbf{k}_{\parallel}) (iH_P(\mathbf{k}_{\parallel}))^{\phi_g} u_g(\mathbf{k}_{\parallel})^\dagger = iH_P(g\mathbf{k}_{\parallel}), \quad g \in G, \quad (\text{VII.15})$$

for the Hermitian Hamiltonian $iH_P(\mathbf{k}_{\parallel})$. Remarkably, antisymmetries with $c_g = -1$ behave as the corresponding symmetries with $c_g = 1$. Therefore, the imaginary-line-gapped Hamiltonian is classified by the K -group $\phi K_G^{(\tau, c_{\text{triv}})+0}(T^{d-1})$ with the trivial homomorphism $c = c_{\text{triv}}$, i.e., $c_{\text{triv}, g} = 1$ for all $g \in G$. This is nothing but the Thom isomorphism [98]

$$\phi K_G^{(\tau, c)+1}(T^{d-1} \times I, T^{d-1} \times \partial I) \cong \phi K_G^{(\tau, c_{\text{triv}})+0}(T^{d-1}). \quad (\text{VII.16})$$

To summarize, in the absence of antisymmetry ($c_g \equiv 1$), we have the exact sequence

$$\phi K_G^{\tau+0}(T^{d-1}) \xrightarrow{\text{im } f_{L_i}^{\text{bdy}}=0} \phi K_G^{\tau+1}(T^{d-1}) \xrightarrow{f_0^{\text{bdy}}} \phi K_G^{\tau+1}(T^{d-1})^{\oplus 2}. \quad (\text{VII.17})$$

The triviality of $f_{L_i}^{\text{bdy}}$ implies that all the nontrivial gapless boundary Hamiltonians involve spectral flow. In the presence of antisymmetries ($\exists g \in G, c_g = -1$), we have

$$\phi K_G^{(\tau, c_{\text{triv}})+0}(T^{d-1}) \xrightarrow{f_{L_i}^{\text{bdy}}} \phi K_G^{(\tau, c)+1}(T^{d-1}) \xrightarrow{f_0^{\text{bdy}}} \phi K_{G_0}^{\tau+1}(T^{d-1}). \quad (\text{VII.18})$$

Since the boundary Hamiltonian $\hat{H}(\mathbf{k}_{\parallel})$ hosts a detachable boundary state when the corresponding point-gapped Hamiltonian may have an imaginary line-gap, this equation implies that $\hat{H}(\mathbf{k}_{\parallel})$ may host a detachable boundary state ($[\hat{H}(\mathbf{k}_{\parallel})] \in \text{im } f_{L_i}^{\text{bdy}}$) if and only if one can open a gap in the boundary state ($[\hat{H}(\mathbf{k}_{\parallel})] \in \ker f_0^{\text{bdy}}$) in $\hat{H}(\mathbf{k}_{\parallel})$ by ignoring the antisymmetries.

The relationship with Wannier localizability is as follows. It was argued that if the d -dimensional bulk admits exponentially localized Wannier states for both occupied and unoccupied states, no spectral flow arises in the boundary Hamiltonian for any

boundary geometry [17]. Therefore, the existence of spectral flow in the boundary indicates that either occupied or unoccupied states are not Wannier localizable. To see this in K -theory, let us introduce the bulk-to-boundary map $f_G^{\text{BBC}} : \phi K_G^{(\tau,c)+0}(T^d) \rightarrow \phi K_G^{(\tau,c)+1}(T^{d-1})$, which sends the bulk Hamiltonian $H(\mathbf{k})$, classified by the degree-0 K -group $\phi K_G^{(\tau,c)+0}(T^d)$, to the boundary Hamiltonian $\hat{H}(\mathbf{k}_\parallel)$. The bulk-to-boundary map $f_{G_0}^{\text{BBC}} : \phi K_{G_0}^{\tau+0}(T^d) \rightarrow \phi K_{G_0}^{\tau+1}(T^{d-1})$ in the absence of antisymmetry is also defined, and forgetting antisymmetries defines the homomorphism $f_0^{\text{bulk}} : \phi K_G^{(\tau,c)+0}(T^d) \rightarrow \phi K_{G_0}^{\tau+0}(T^d)$ for the bulk. We obtain the following commutative diagram in which the second line is exact:

$$\begin{array}{ccccc} \phi K_G^{(\tau,c)+0}(T^d) & \xrightarrow{f_0^{\text{bulk}}} & \phi K_{G_0}^{\tau+0}(T^d) & & \\ & & \downarrow f_G^{\text{BBC}} & & \downarrow f_{G_0}^{\text{BBC}} \\ \phi K_G^{(\tau,c_{\text{triv}})+0}(T^{d-1}) & \xrightarrow{f_{L_i}^{\text{bdy}}} & \phi K_G^{(\tau,c)+1}(T^{d-1}) & \xrightarrow{f_0^{\text{bdy}}} & \phi K_{G_0}^{\tau+1}(T^{d-1}) \end{array} \quad (\text{VII.19})$$

Given a bulk Hamiltonian $[H(\mathbf{k})] \in \phi K_G^{(\tau,c)+0}(T^d)$, the existence of spectral flow in the boundary means $f_G^{\text{BBC}}([H(\mathbf{k})]) \notin \text{im } f_{L_i}^{\text{bdy}} = \ker f_0^{\text{bdy}}$. The commutativity of the diagram implies $f_{G_0}^{\text{BBC}} \circ f_0^{\text{bulk}}([H(\mathbf{k})]) \neq 0 \in \phi K_{G_0}^{\tau+1}(T^{d-1})$. This means that the bulk topological invariant without antisymmetry, which detects the element of the K -group $K_G^{\tau+0}(T^d)$ signaling the boundary spectral flow, should provide the obstruction of Wannier localizability.

VIII. REFLECTION-INVARIANT TOPOLOGICAL CRYSTALLINE INSULATORS

Our formulation is also applicable to topological crystalline insulators. As a prime example, we study a two-dimensional topological insulator with commutative chiral and reflection symmetries [99–101]:

$$\Gamma H(k_x) \Gamma^{-1} = -H(k_x), \quad \mathcal{R}_+ H(k_x) \mathcal{R}_+^{-1} = H(-k_x), \quad (\text{VIII.1})$$

with unitary matrices Γ and \mathcal{R}_+ satisfying

$$\Gamma^2 = \mathcal{R}_+^2 = 1, \quad [\Gamma, \mathcal{R}_+] = 0. \quad (\text{VIII.2})$$

At a reflection-invariant edge, a gapless state

$$H_{\text{AIII}+\mathcal{R}_+}(k_x) = k_x \sigma_x \quad (\text{VIII.3})$$

appears. This Dirac model in Eq. (I.5) indeed respects these symmetries with $\Gamma = \sigma_z$ and $\mathcal{R}_+ = \sigma_x$.

Notably, this reflection-invariant gapless state exhibits no spectral flow and hence is detachable from the bulk, similarly to the Dirac surface state protected by chiral symmetry. To confirm this, we couple it to a trivial band $\varepsilon \sigma_x$ ($\varepsilon \geq 0$) by

$$\tilde{H}_{\text{AIII}+\mathcal{R}_+}(k_x) = \begin{pmatrix} k_x \sigma_x & v \sigma_- \\ v \sigma_+ & \varepsilon \sigma_x \end{pmatrix}, \quad (\text{VIII.4})$$

with the coupling strength $v \geq 0$. This four-band model remains to respect chiral symmetry with $\Gamma = \sigma_z$ and reflection symmetry with $\mathcal{R}_+ = \text{diag}(\sigma_z, 1)$. Similarly to the chiral-symmetric two-dimensional Dirac model studied in Sec. IC, the four energy bands are obtained as

$$\sqrt{2}E(k_x) = \pm \sqrt{k_x^2 + \varepsilon^2 + v^2 \pm \sqrt{(k_x^2 - \varepsilon^2 + v^2)^2 + 4\varepsilon^2 v^2}}, \quad (\text{VIII.5})$$

exhibiting a global gap in Eq. (I.21). Since gap-opening perturbations can further be added away from reflection-invariant corners, this also implies the emergence of corner states at zero energy [102].

Corresponding non-Hermitian systems $H_{\text{AIII}+\mathcal{R}_+}(k_x)$ respect chiral symmetry and commutative reflection symmetry:

$$\Gamma H_{\text{AIII}+\mathcal{R}_+}^\dagger(k_x) \Gamma^{-1} = -H_{\text{AIII}+\mathcal{R}_+}(k_x), \quad \mathcal{R}_+ H_{\text{AIII}+\mathcal{R}_+}(k_x) \mathcal{R}_+^{-1} = H_{\text{AIII}+\mathcal{R}_+}(-k_x), \quad [\Gamma, \mathcal{R}_+] = 0 \quad (\text{VIII.6})$$

Their point-gap topology is captured by the zeroth Chern numbers of the Hermitian matrix $i[H_{\text{AIII}+\mathcal{R}_+}(k_x) - E_P] \Gamma$ at reflection-invariant momenta. In the presence of an imaginary line gap, by contrast, $iH_{\text{AIII}+\mathcal{R}_+}(k_x)$ hosts two pairs of independent zeroth Chern numbers depending on $\Gamma = \pm 1$. Consequently, the point-gap topology is of extrinsic nature, underlying the detachment of reflection-invariant corner states.